Investigation of a Novel Decision Support Metric for Head and Neck Adaptive Radiation Therapy (ART) using a Real-Time In-Vivo Portal Dosimetry System

By

Seng Boh Lim

A Dissertation Submitted

In partial fulfillment of the Requirements for the Degree of

Doctor of Philosophy

in

Biomedical Informatics

Department of Health Informatics Rutgers, The State University of New Jersey

School of Health Professions

August 2019

Final Dissertation Defense Approval Form

Investigation of a Novel Decision Support Metric for Head and Neck Adaptive Radiation Therapy (ART) using a Real-Time In-Vivo Portal Dosimetry System

by

Seng Boh Lim

Dissertation Committee:

Fredrick Coffman PhD

Suril Gohel PhD

Nancy Lee MD

Dale Michael Lovelock PhD

Approved by the Dissertation Committee:

_____ Date: _____

_____ Date: _____

_____ Date: _____

_____ Date: _____

_____ Date: _____

Table of Contents

List of Figures

List of Tables

Abstract

In adaptive radiation therapy (ART) of head and neck cancer, any significant anatomical changes observed are used to adapt the treatment plan to maintain target coverage without elevating the xerostomia risk. However, the additional resources required for ART pose a challenge for broad-based implementation. It is hypothesized that the transit fluence change is associated with volumetric change in the vicinity of the target and therefore can be used as a decision support metric (DMS) for ART. This was evaluated by comparing the fluence with volumetric changes in twenty-four patients. Transit fluence was measured by an in-vivo portal dosimetry system (RTPD). Weekly cone beam computed-tomography (CBCT) was used to determine volume change in the rectangular region of interest (ROI) from condyloid process to C6. The integrated fluence through the ROI and the salivary glands (SG) on the day of the CBCT scan was calculated with the first treatment as the baseline. The correlation between fluence and volume changes was determined. Logistic regression was also used to associate the 5% ROI volume reduction replanning trigger-point and the fluence change. The model was assessed by a chi-squared test. The area (AUC) under the receiver operating characteristic curve (ROC) was also determined. The xerostomia risk was assessed by the scores change of the patients' MD Anderson Dysphagia Inventory (MDADI). The association of the MDADI with age, gender, mean dose to SG, weight, volumetric and fluence changes were assessed using Spearman rank-correlation. A total of 108 pairs of CBCT and RTPD measurements were obtained. The correlation between fluence and volumetric changes were found to be -0.837 (p-value<0.001). The AUC of the ROC was found to be 0.91. The correlation between

SG-specific fluence and volumetric changes was found to be -0.62 (p-value<0.001). Twenty-one patients responded to the MDADI. Fluence and volumetric changes were found to have association with the physical, functional and total MDADI changes. No significant association with age, gender, and weight change were found. A transit fluence based DSM is not only a viable alternative to serial CBCT in assisting clinicians in the patient selection, but also lowers the resource barrier of ART implementation.

Keywords: Transit dosimetry, Head and Neck Cancer, Xerostomia, Adaptive Radiation Therapy, Automation

Chapter 1

Introduction

Xerostomia is a devastating late effect of head and neck cancer (HNC) radiation therapy[1]. Because of the proximity of the salivary glands to the tumor site, they may overlap with the planning target volume (PTV) that receives prescription dose, thus radiation exposure to the glands is often unavoidable. Advanced radiation delivery techniques, such as intensity modulated radiotherapy (IMRT)[2] and volumetric modulated arc therapy (VMAT), are used to maximally spare surrounding normal tissues [2,3] while delivering the prescription dose to the PTV. Even with these techniques, significant toxicity reduction to the salivary glands and xerostomia risks are still observed [4,5]. During a course of a radiation therapy, an HNC patient can experience significant anatomical changes. Factors such as tumor shrinkage, weight loss, and body fluid redistribution[6] and possible shifts of the parotid glands (PG) towards the high dose region[6] can result in an unexpected dose increase to the PGs and higher risk of xerostomia[1,7,8].

Adaptive radiotherapy (ART), the adaption of the treatment plan to account for such anatomical changes[6,9-12] is the only clinical strategy that is able to maintain both the PTV coverage and sparing of the organ at risk (OAR) throughout the treatment course.

Implementation of ART is a significant clinical challenge. Although dosimetric measures such as the mean PG dose and normal tissue complication probability are very effective in predicting high grade xerostomia [8,13-15], Van Dijk[16,17], Belli[18], Sanguineti[19] and You[20] find that they are not effective predictors for acute xerostomia during normal

fractionated 54-70 Gy treatments. Volumetric changes determined from parotid gland contours[16,18,19,21] and neck separation[20] and are found to be stronger and earlier predictors. At 6-12 months follow-up, it is found that the early PG volumetric changes during treatment are associated with late xerostomia[16]. Volumetric changes are also believed to be more strongly associated with stem cell sterilization[22], than dosimetric metrics[16]. Three-dimensional Imaging procedures[6,9-11,23,24], such as cone beam computed tomography (CBCT) and magnetic resonance imaging (MRI), performed on a regular basis throughout the treatment course can be used to capture anatomical changes. This technique has been shown to be effective in reducing dose to the PGs[6,9,11]. However, the additional imaging procedures and physician assessment are time consuming and costly, thus hindering ART from being more broadly implemented[6]. As the scans are taken only weekly, there is potential that the best time point to adapt has been missed. Furthermore, Significant variability in the timing of anatomic change during a treatment course among patients is observed[16,25]

Electronic portal image detector (EPID) dosimetry systems that use exit radiation, or transit fluence, from patients during treatments have been investigated and implemented for both real-time and offline in-vivo delivery monitoring[26-29]. Such approaches compare the transit fluence detected by the EPID with the transit fluence expected based on the treatment plan. The results are used as a daily quality assurance of the delivery process and of patient safety. No additional patient exposure or significant workload for the therapists is incurred.

The relationship between the change of transit fluence (ϕ) and the anatomy change in patients over the course of treatment has not been investigated. If established, such a relationship could be used to provide a daily signal to the clinic replacing the routine CBCT at very low cost that anatomic change in the treated tissues was occurring and the need for plan adaptation should be reviewed.

1.1 Goals and Objectives

To achieve the goal of using EPID in monitoring HNC patients during treatment, eight objectives were established and are listed in the followings.

1.1.1 To identify a DSM to analyze transit fluence

The first objective is to determine a DSM that can be used to track the volumetric changes of HNC patients.

1.1.2 Phantom Study

Before using the DSM in the clinic, the DSM should be tested in a phantom study to demonstrate its sensitivity.

1.1.3 To Obtain IRB Approval for a Clinical Study

An IRB application is submitted for the patient study prior as human subjects are involved.

1.1.4 Phase 1 Clinical Study

After establishing the sensitivity, the DSM should be tested with five patients in a clinical setting to assess the usability.

1.1.5 Phase 2 Clinical Study

After successfully completed and reviewed the results of phase 1 study, an additional 21 patients will be used to assess the effectiveness of the DSM.

1.1.6 To Assess the Ability of the DSM to Predict the Adaptation Point of ART

To improve the clinical workflow, it is beneficial to understand the predictability of ART adaptation point with the proposed DSM.

1.1.7 Implementation of Salivary Glands Specific DSM

A salivary gland specific DSM, DSM_{sg}, using the projection of the three-dimensional salivary glands contour and the treatment field apertures, will be implemented and calculated on the patient data.

1.1.8 To Assess the Predictability of the Xerostomia with the DSM

The risk association between xerostomia and the salivary gland specific DSM will be examined.

1.2 Research Hypothesis

In this study, there are three hypotheses.

1. It is hypothesized that the change in transit fluence is associated with volumetric change in local anatomy, which is a decision support metric (DSM) in the ART process. This hypothesis is evaluated by comparing change in transit fluence with the change in the irradiated volume in HNC patients.
2. It is hypothesized that the DSM can be used to as a signal to the clinicians for taking replanning action of ART;
3. It is further hypothesized that the change of transit fluence captured by DSM_{sg} is associated with the changes in dose deposition in the salivary glands and the dose change is associated with the risk of xerostomia.

1.3 Abbreviations

ART	Adaptive radiotherapy
AUC	Area under the curve
β_0	Constant term of the logistic regression
β_1	Coefficient of an input parameter of the logistic regression
CBCT	Cone beam computed tomography
CI	Confidence Interval
CT	Computed tomography
DSM	Decision support metric
EPID	Electronic portal image detector
FPR	False positive rate
ϕ	Transit fluence
$\Delta\phi$	Change of transit fluence
$\phi_{e,o}$	Baseline transit fluence of pixel e
$\phi_{e,i}$	The i^{th} session transit fluence of pixel e
ϕ_e	Integrated transit fluence of pixel e
$\Delta\phi_{e,i}$	The change of ϕ_e of any session i
$< \Delta\phi_{e,i}>$	average change of ϕ_e of any seession i
HNC	Head and neck cancer
h	Height of the cylinder representing the neck in the ROI
IMRT	Intensity modulated radiotherapy

M120	Millennium 120
MDADI	MD Anderson Dysphagia Inventory
MLC	Multi-leaf collimator
MRI	Magnetic resonance imaging
MV	Megavoltage
OAR	Organ at risk
OR	Logarithmic odds ratio
P_i	Probability of replanning at session i
PG	Parotid gland
PTV	Planning target volume
R	Radius of the half sphere representing the head in the ROI
r	Radius of the cylinder representing the neck in the ROI
Δr	The change of the radius of the cylinder in the ROI
ρ	Spearman rank correlation
ROI	Region of interest
ROC	Receiver operating characteristic
SSD	Source to detector distance
SG	Salivary glands
TPS	Treatment planning system
TPR	True positive rate
VMAT	Modulated arc therapy
V_{ROI}	The volume of the ROI

$\Delta V_{ROI,i}$	The volumetric change of the ROI at session i
WD	Watchdog system
Δweight	Patient weight change

1.4 Importance of the Study

Figure 1 shows an example of the significant reduction in volume of an HNC patient between the first day and the last day treatment. As a result, significant dose increase to OAR can occur. In ART, regular imaging is used to monitor the patients' anatomical changes to capture the accurate point of replanning to remedy this challenge.

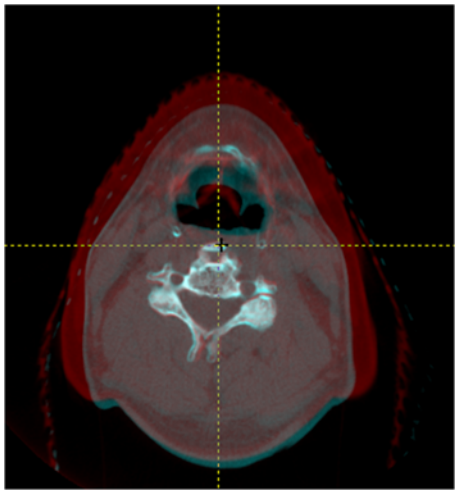

Figure 1: shows the anatomical change of a patient between the first day treatment (red) and the last day of treatment(blue). Significant reduction in volume can be observed.

Unlike other imaging modalities, performing frequent imaging with transit fluence (ϕ), which is the exiting radiation of treatment fields from patient bodies, does not increase the patient radiation exposure or additional time to the clinical workflow. This provides more opportunities to capture the optimal adaption time. However, the relationship between the change of ϕ and the anatomy change in patients over the course of treatment has not been investigated. This study intends to define and characterize a transit fluence based DSM

that can predict the replanning action point for ART through phantom and clinical testing. The association to xerostomia will also be studied to evaluate the DSM predictability. Because of the simplicity of the DSM, the results of this study can easily be automated and incorporated in the normal treatment workflow not only to provide the replanning signal to clinicians but also promote the implementation of ART.

Chapter 2

Literature Review

Xerostomia is the subjective feelings of dry mouth is associated with the reduction of saliva flow in a person's mouth[30,31]. Patients, who suffer from this condition, can experience discomfort ranging from soreness, burning, loss of taste, and difficulty in swallowing[30], resulting in a significant reduction on the quality of life[8-12,30,31]. The identification of the condition usually relies on self-reporting surveys as the measure of saliva is not easily obtained[30,31].

Saliva is produced in the salivary glands located in the head and neck region. The three main sites responsible for salivary production are the parotids, submandibular, and sublingual glands[1,30]. There are also minor salivary glands distributed in the oral cavity and pharynx regions[1].

The cause of xerostomia can be attributed to pharmacological side effects, systemic diseases, physiological changes, psychological changes, radiation therapy or the combination of the above factors[30,32]. Radiation-induced xerostomia, which is often a side effect of HNC radiation treatment, is the primary focus on this review. HNC describes the cancers, such as Hodgkin's disease and non-Hodgkin's lymphoma, that occurs in the head and neck region[1]. Radiation therapy, which delivers high energy ionizing x-ray to the tumor site, is one of the main treatment modalities for HNC. A course of radiation therapy treatment usually takes several weeks of daily treatments to complete. Xerostomia is often observed in HNC patients post radiation treatments. It is found to be associated with the

amount of radiation dose received by the salivary glands[1,7]. In this article, the cause, identification method and strategies of reducing the risk of radiation-induced xerostomia will be reviewed.

2.1 Method

Literature search is performed using PubMed and Web of Science using the keywords "radiation therapy" and "Xerostomia". The background information, prevalence, anatomical structure, etiology, and measurement techniques for xerostomia, are assessed. Articles with radiation-induced xerostomia and ART are selected for review. The gender mix, treatment modality, xerostomia identification method, potential predictor and monitoring methods are reviewed.

2.2 Results

2.2.1 Prevalence

Xerostomia is defined as a subjective complaint of dry mouth by a patient and is associated with the reduction saliva production[30-32]. It is estimated that this condition affects 17 to 29 percent of the population. Women generally have higher prevalence[30]. About 40% of HNC patients, who receive radiation therapy, experience radiation-induced xerostomia [22]. As saliva plays an important role in digestion, speech, and disinfection [1], the reduction of saliva can significantly affect the quality of life (QoL) and increase risk of oral fungal infection [1,31].

2.2.2 Anatomical Structure

Saliva is secreted from major and minor salivary glands located in the head and neck region via a network of ductal system into oral cavity[1,22,33,34]. Major salivary glands are comprised of parotid, submandibular and sublingual glands. Minor glands, which have significant patient specific variation, distribute throughout the oral cavity[1,33,34]. In terms of saliva production, about 82 to 95% is produced by the three major salivary glands. Parotids constitute about 60-65% of the production. About 20-30% is produced by submandibular glands[1]. A normal human produce about 1.0 to 1.5L per day of saliva[1,34].

Serous and mucous secretions are the two types of fluid making up saliva. Serous secretion is produced mainly in acinar acini found in the parotids. The minor glands are mucous acini that secrete mucous only. Submandibular and sublingual glands, which contain both acinar and mucous acini, produce a mixture of serous and mucous secreations[1,22,34].

2.2.3 Etiology

Pharmacological, autoimmune disorder, systemic disease, and radiation exposure can cause salivary gland acinar destruction resulting in xerostomia [1,30,31,35]. The symptom of dry mouth is a common side effect of prescription medications. Although the rate of reporting is not well defined, the severity is usually associated with the dosage of the underlying drug. As people tend to take more medications with aging, the risk of elderly is also higher[30]. Lymphocytic infiltration of the exocrine glands, including salivary glands, is characteristic process of an autoimmune disorder called Sjogren's Syndrome. The

destruction of the salivary and lacrimal glands result in dry mouth and eyes[36]. Other diseases, such as human immunodeficiency virus infection, amyloidosis, and diabetes, can also cause the destruction of salivary glands [1,30,32,35,36].

Radiation-induced xerostomia occurs when salivary glands are exposed to ionizing radiation. Based on animal studies[37,38], the mechanisms are different in the low and high radiation dose. At low dose, apoptosis, resulted from double strand break of the DNA[39], is the main cause. Cell death at high dose is usually characterized by radiation necrosis. With the standard target prescription of 50-70Gy, salivary function is reported to decrease between 60% to 90% after salivary glands are exposed to a radiation dose of 26-39 Gy[22]. Serous acinar cells are considered to be more radiosensitive than mucous cells[1,22,40]. To reduce xerostomia, lower dose limit is typically set to parotids[8]. In clinical practice, the salivary glands are found to be more radiosensitive than expected. Radiation-induced sterilization of stem cells around the salivary glands, preventing the repair and renewal of the salivary glands, is suggested to be cause[22]. Because of the higher radiosensitivity and saliva production, parotids are usually considered as the OAR[41] when a radiation treatment plan is designed. Submandibular glands, the second largest saliva producer, are suggested to be included in the OAR consideration[15].

2.2.4 Measurement of Radiation Induced Xerostomia

Radiation-induced xerostomia is often assessed with histological assessment, saliva output, imaging, dose response and questionnaire[1,33,35,42].

2.2.4.1 Histological Assessment

Histological assessment of salivary function involves invasive procedure of neck dissection [33,43] to assess the cellular structure of the salivary glands. Because of the relative high risk, this is usually performed in predominantly animal studies[1,33]. In a human study, Teshima[43] studies the histological change in salivary glands after radiation therapy (RT) with a cohort of 6 patients. With 30Gy of radiation, a significant loss of acinar cells in parotids are observed. The acinar cells in submandibular glands do not demonstrate the same amount of damage. The significant loss of parotid volumes observed in CT and the functional loss of saliva flow using Saxon Test[44] are also observed which are attributed to the acinar cells damage. The structural changes in human are found to be comparable to the findings in the animal studies. A strong correlation between the change of CT signals and the adipose ratio is also observed[43].

2.2.4.2 Sialometry

Sialometry is an objective measure of the saliva flow within a given amount of time[33,35]. Reproducibility is a challenge in sialometry. Saliva flow of a person vary significantly for an individual depending on the hydration condition, simulation, simulation and posture[13,44,45]. Navazesh[45] provides a guideline of the preparation and test performance of the sialometry attempting to minimize the variation. A typical standardized test can take between 7 to 10 minutes to perform[45]. However, the correlation between the absolute saliva output and xerostomia is found to be weak[13,35] which can be attributed to the low

reproducibility of sialometry. Chao[13] finds the standard deviation of saliva output is in the order of 20-30%.

2.2.4.3 Imaging

Imaging is often used to assess the functionality of salivary glands. The accuracy, specificity, cost, patient risk and time are important factors that determine the imaging modality[33,42].

2.2.4.3.1 Magnetic Resonance Imaging (MRI)

MRI is a non-ionizing radiation imaging technique. It utilizes the interaction of the proton density and spin relaxation time of tissues compounds with a strong external magnetic field to delineate different tissues[46]. Superconducting magnets are often used to generate the strong magnetic field. Because of the superior soft tissue contrast over CT, it is a very useful tool in evaluating head and neck patients[33,42]. Nomayr[47] is able to observe radiation induced parotid and submandibular glands shrinkage using MRI.

2.2.4.3.2 Ultrasonography (USG)

USG uses high frequency sound wave, in the range of 2-10 MHz, to delineate tissues. When the sound wave hits different tissues, it will be bounced back (Echo). By analyzing the time and direction of the echo, the structural information can be displayed[46]. Superficial soft tissues and organs, such as thyroid and salivary glands, can be delineated[33,42]. It is shown to be valuable and used extensively in evaluating salivary

glands and diagnosing Sjogren's Syndrome[48]. However, it is not widely used for assessing radiation induced xerstomia[33].

2.2.4.3.3 Sialography

Sialography is mainly used for chronic sialadenitides to examine the ductal structure of the salivary glands[33]. It can be performed using x-ray or MRI[33,42]. X-ray based sialography involves injecting contrast agent into the salivary ductal structure to improve visibility when the images are taken. CT is usually used to provide three-dimensional information[42]. Unlike x-ray based sialography, MRI based sialography does not involve ionizing radiation or contrast agent injection. It uses T_2W sequence to provide the three-dimensional ductal information[33,49]. To monitor the radiation induced changes to the salivary ductal system, repetitive tests would be required[49].

2.2.4.3.4 Computed Tomography (CT)

CT is the standard equipment in most radiology department. Imaging salivary glands with CT is relatively easier, cheaper and faster than MRI[42]. It uses ionizing radiation to acquire the images. Because of the lower soft tissue contrast, contrast agent is often used to improve the visibility of the salivary glands. Similar to the Sjogren's Syndrome, fatty tissues deposit are observed at the post radiation salivary glands and the corresponding changes in the CT value are observable without using contrast[33,36,43].

2.2.4.3.5 Positron Emission Tomography (PET)

A positron is a positive charged electron emitted by radioactive isotopes. These isotopes are incorporated into compounds, such as ^{18}F-fluorodeoxyglucose (^{18}FDG), which can be administered to patients and metabolically processed by the targeted tissues or organs[46,50]. Patients are placed in a PET scanner which comprised of an array of gamma cameras to capture the positron emitting from the body. These signals are processed to generate the three-dimensional image of the radiation activity corresponding to the metabolic function of the targets[42,50]. The post radiation therapy functionality change of salivary gland has also been shown to associate with the signals of ^{18}FDG PET[51,52].

2.2.4.3.6 Scintigraphy

Similar to PET, scintigraphy requires administration of radioactive isotopes to assess the functionality of the targeted tissues or organs. The typical agent used for salivary glands assessment is ^{99m}Tc isotope[33,42,46]. It is restricted to two-dimensional information. The low spatial resolution and sensitivity may not be suitable to assess salivary function[33,42].

2.2.4.4 Dose Response

Normal tissue complication probability (NTCP) is the empirically fitted toxicity probability of a tissue after uniform radiation with clinical data[53]. Lyman-Kutcher-Burman (LKB)[53,54] NTCP is the scheme widely used in data fitting. The mean dose of the parotid glands, $<Dose_{PG}>$, because of the saliva production contribution and radiosensitivity, are

often used as the predictor of xerostomia[7,11,35,55,56]. Grade 4 xerostomia, as defined by Radiation Oncology Group (RTOG)/European Organization for Research and Treatment of Cancer (EORTC)[57], is associated with <$Dose_{PG}$> between 26 to 39 Gy. To avoid xerostomia, Daesy[8] recommends at least one parotid should be spared with a mean dose of 20 Gy or less. The mean dose should be kept below 25 Gy if both parotids are spared. A large study of 222 patients show that <$Dose_{PG}$> is capable to predict grade 4 xerostomia saliva flow reduction using LBK NTCP[7]. However, a recent study by Gabrys[58] indicates that <$Dose_{PG}$> has a limitation in predicting lower grade xerostomia. Significant variations between xerostomia and the predicted risk from NTCP are also observed[8,20,25,35,59]. Other dose deposition in submandibular glands should also be considered in the risk reduction of xerostomia[60]. Because of the complexity of radiation induced xerostomia, physical models are unlikely to account of all the contributing parameters[35].

2.2.4.5 Grading and Questionnaire (G&Q)

MD Anderson Dysphagia Inventory (MDADI) is the first clinical validated questionnaire[61] to assess the subjective quality of life of head and neck patients[62-64]. The questionnaire is comprised of twenty questions with scores 1 to 5. It covers quality of life (QoL) of the patients through four subsets: global, emotional, functional and physical. Globel subset uses a single question to assess the underlying affecting the patients. Emotional, functional, and physical use multiple questions to assess the assess the affectiveness from the condition, swallowing effectiveness and self-perceived of the condition. The RTOG/EORTC[57] is another grading system that is also widely used by clinicians to provide a qualitative assessment of xerostomia of HNC patients[1]. This system

classifies xerostomia into five grades of severity ranging from 0 being no observable to 5 being death related to RT. Details of a patient, such as the subjective perception of the condition, is not part of this system. A more comprehensive assessing system for Late Effects of Normal Tissues (LENT) focusing on the several inter-dependent factors: Subjective, Objective, Medical management and Analytic (SOMA)[65]. Under this system, both assessments from patients and clinicians, subjective and objective information, are recorded. The actions taken to remedy the symptoms and analytical tools used are also documented. Several studies have shown that LENT/SOMA is a more effective tool than RTOG/EORTC scale to identify radiation-induced xerostomia[66-69]. During the development of the third edition of Comprehensive Grading System for the Adverse Effects of Cancer Treatment (CTCAE v3.0)[70], LENT/SOMA is incorporated into the framework[67,70]. To document the post RT progression of the xerostomia, improvements to the grading system reflecting the longitudinal changes are suggested[35].

2.2.5 HNC Radiation Therapy

Because of the close proximity of the salivary glands to the tumor site, typically referred to as the primary target volume (PTV), radiation exposure to the glands are sometimes unavoidable. About 40% of HNC patients suffer from late effect xerostomia. To lower the risk of xerostomia, Deasy et al[8] recommends sparing at least one parotid. If both parotids are exposed, the mean dose spared to less than 20Gy can reduce the risk of severe xerostomia as described in the earlier section. In a recent study, Hawkins[14] suggests that the dose to salivary glands should be kept as low as possible to reduce the risk.

With the advances in radiation delivery, IMRT[2] and VMAT[71] are the current standard care for radiation therapy. By using multi-leaf collimators (MLC) on the treatment machines and an inverse treatment planning system, high radiation dose gradient can be generated to deliver the desired prescription dose to the PTV and spare the surrounding normal tissues [2,3]. These techniques are also applied to HNC[6] [72] to achieve sufficient dose to PTV for local control and significant reduce toxicity to the salivary glands and xerostomia risks[4,5].

During the treatment course of a radiation therapy, a patient can experience significant anatomical changes, typically shrinkage around the neck, resulting in a treatment deviation from the original plan[6,9,11,15,23,73-76]. These changes often involve multiple factors such as tumor shrinkage, weight loss, and body fluid distribution[6] resulting in significant dose change to the PTV and the OAR[6]. It is also observed that the PG tend to shift towards the high dose region[6] resulting in unexpected dose increase to PGs and higher risk of xerostomia[1,7,8].

2.2.5.1 Adaptive Radiotherapy (ART)

ART is proposed to adapt the treatment plans with the anatomical changes[6,9-12] ensuring the PTV coverage and sparing the OAR. In a twenty-patient study, Nishi[76] finds there is a clear benefit of reducing xerostomia risk with ART. To maximize the benefit of ART, monitoring and dose reduction of the OAR is the best strategy[9]. Fifteen articles that assess radiation therapy induced xerostomia between 2005 to 2017 are identified.

2.2.5.2 Gender

About 64% to 95% of cohorts from the studies are males. This can be related to the availability of the patients. As a result, the result and conclusion can be biased towards males.

2.2.5.3 Treatment Technique

IMRT and VMAT are the current standard care for HNC radiation treatment. In the existing paper, all treatments are treated with IMRT. The treatment planning quality between IMRT and VMAT are considered similar[77,78]. The experience from IMRT can likely be transferred to VMAT treatments.

2.2.5.4 Xerostomia Identification

Saliometry[43], histology[43], G&Q[14,15,17-21,25,59,76,79], and NTCP[9,11,25] methods are used in the articles to identify xerostomia. The timing varies from immediate to 12 months post radiation. The severity of xerostomia also varies from low grade to severe. Because of the different reporting metric, quantitative comparison among articles with different measurement metric can be difficult. Several authors use two or more techniques to correlate the objective to the subjective results[14,15,17-21,25,43,59,76,79]. The end points of these studies also vary from grade 1 to grade 4.

2.2.5.5 Predictors

Several predictors are shown to help identifying suitable patients for ART before treatment. Castelli[11] investigated the correlation between PG overdose (the risk of xerostomia) and the images from the weekly CT during treatment. A statistically significant risk in xerostomia ($p<0.001$) is correlated with the PG volume from the weekly CT. Brown[10] investigated the potential predictors, such as initial weight, nodal size and diagnosis, and identified the initial weight as a strong predictor for replanning using logistic regression. Machine learning method has also been explored to identify potential predictors for patient selection[12]. However, these models are unable to predict or identify the timing of replanning as significant variation among patients are observed[17,25]. $<Dose_{PG}>$ and NTCP are very effective in predicting high grade xerostomia prior to treatment[8,13-15]. However, Van Dijk[17] and You[20] find the $<Dose_{PG}>$ is not an effective predictor for xerostomia during treatment. This seems to indicate the insensitivity of dose metric to individual variation of radiation induced xerostomia. Volumetric changes, such as neck separation[20] and parotid gland contours[17,21], are found to be a stronger predictor.

A patient's anatomy, during the course of treatment, is monitored to capture any significant changes through regular imaging [6,9-11,23,24]. When a significant volumetric change, resulting from anatomical change, is observed, a new ART plan is designed with the latest anatomical information to maintain the objectives of maintaining tumor prescription and minimize the dose to normal tissues. This technique has been shown to be effective in reducing dose to the PGs[6,9,11].

2.2.5.6 Monitoring

To monitor the anatomical changes, additional imaging procedures, such as weekly CT, CBCT and MRI, are performed on a regular basis[6,7,9-11,23]. These resulting image sets are assessed by physicians to determine if ART is necessary. The additional imaging procedures and assessment can be time consuming which hinder the ART from being broadly implemented[6]. PGs are typically used as the proxy of all salivary glands and the dose deposition as the risk assessment of xerostomia. The effectiveness of using other salivary glands have not been explored.

2.2.5.7 Transit Fluence Monitoring

EPID dosimetry system, that uses exit radiation from patients during treatments has been investigated and implemented for both real-time and offline in-vivo delivery monitoring[26-29]. These systems use exit radiation from patients during treatment. No additional radiation or time burden are incurred on the patients. As these systems are designed for the quality assurance of the patient safety and overall dosimetric delivery, the systematic relationship between the measured EPID signals, χ or γ metrics[80,81], and the clinical decision metrics, such as dose volume histogram (DVH), of the OARs and PTV [28] are not well established. Rozendaal[27] reconstructed the three-dimensional dose distributions using the back-projected fluence derived from the measured patient exit dose and the planning CT. The results showed that the γ results from this approach have statistically significant correlation with the PTV changes based on a cohort of 20 HN

patients. However, the γ analysis[81] of this approach also is found to be time consuming, 3 to 5 times over-sensitive to corresponding anatomical changes and susceptible to noise.

The transit fluence, ϕ, is the photon leaving a patient during a radiation treatment[29]. The relationships between the change of ϕ and the anatomy change in patients have not been the focus of recent studies. It is possible to track the anatomical changes of the salivary glands and establish the systematic relationship between the observed ϕ changes to the physicians' adaptive planning decision.

2.3 Conclusions

Radiation induced xerostomia is a complex problem. Even with the latest radiation delivery system, a significant amount of HNC patients still suffer from radiation-induced xerostomia. ART is a promising strategy in further reducing risk in xerostomia occurrence in HN radiation therapy and improve the quality of life of HNC patients. The time-consuming aspect in monitoring anatomical changes during treatment is preventing this strategy from achieving a wider implementation. A more efficient monitoring methodology and decision support system can potentially expedite the adoption of ART.

Chapter 3

Methods and Materials

3.1 DSM

The primary photon fluence incident on the patient, support couch and immobilization system is attenuated and scattered before being detected at the EPID (Figure 2).

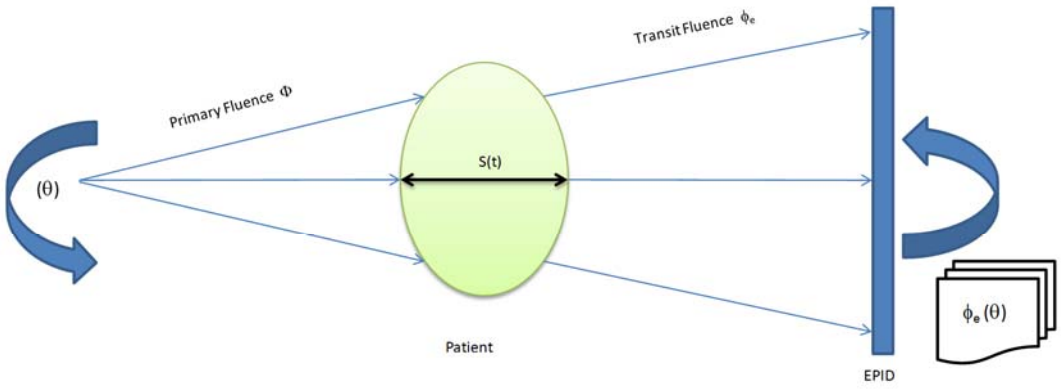

s

Figure 2: A schematic of the photon beam interaction with a patient and transit fluence deposition on the EPID panel.

Note that the transit fluence detected is the sum of the attenuated primary fluence and the scattered fluence. The EPID images were captured by WD in cine mode, typically 3000 to 4000 images per treatment. All the images for a given treatment session were summed across all treatment arcs to give an integrated transit fluence ϕ_e at EPID pixel e. Given a fixed treatment plan and patient's bony anatomy being repositioned perfectly, any change

in ϕ_e at a given treatment can be attributed to anatomical changes in the patient. The change of ϕ_e of any session *i* is defined as

$$\Delta\phi_{e,i} = \phi_{e,i} - \phi_{e,0}$$

where $\phi_{e,i}$ and $\phi_{e,o}$ are the exit fluence of session i and the baseline respectively. The first session of a treatment course is used as the baseline. The objective here is to monitor the change in anatomy in the region of the patients' lower face and neck. A fixed rectangular region of interest (ROI) corresponding to the projection of this region of each patient (Figure 3) on the transit fluence plane was used to calculate the average fluence change $<\Delta\phi_{e,i}>$.

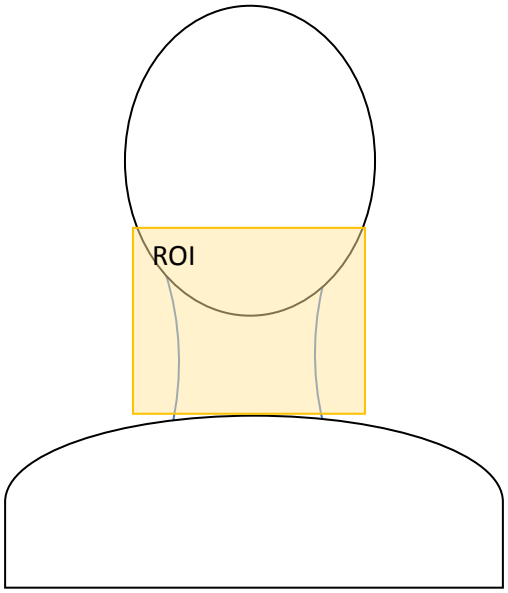

Figure 3: A schematic of a HNC patient with a rectangular regional of interest (ROI) defined around the neck region used in the transit fluence calculation.

3.2 Phantom Study

A thoracic phantom, as shown in Figure 4 , was used to mimic an HNC patient with significant volume loss. It was setup with CBCT on a Varian Truebeam with M120 MLC. A VMAT plan was delivered to the phantom and the corresponding $\phi_{e,i}$ was measured. To measure the baseline transit fluence, $\phi_{e,0}$, the neck region of the phantom was wrapped with a 5mm bolus to model the initial neck volume of an HNC patient, i.e. before volume loss (Figure 4), and the same delivery was given. The fluences in the two cases were converted with MATLAB and transferred to an in-house software to calculate the $< \Delta\phi_{e,i} >$.

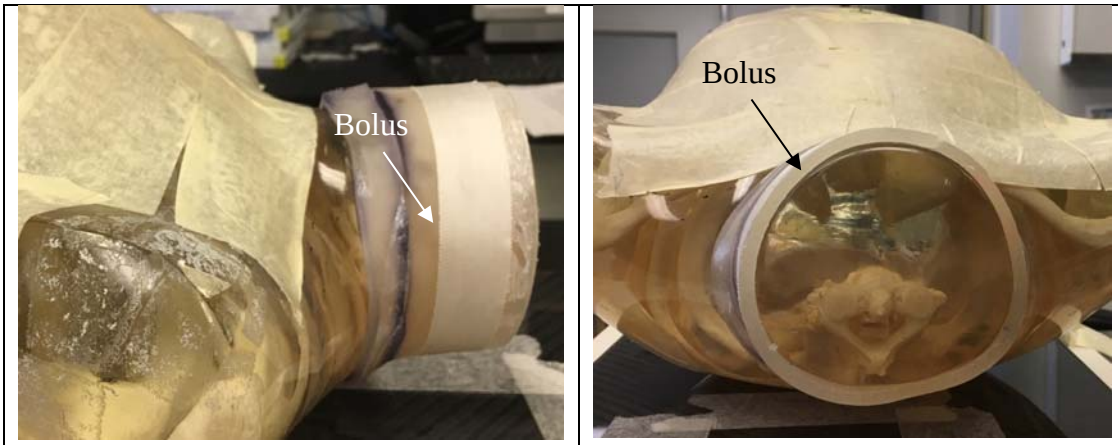

Figure 4: (a) side view of the phantom with a 5mm bolus; (b) shows the axial view of the phantom with the 5mm bolus.

3.3 IRB Approval

IRB approval was applied and approved. The number is 18-257 and the letter was attached in Appendix I.

3.4 Phase 1: Clinical Study

Five HNC patients were recruited for this study. All treatments were delivered with a 6 MV photon beam using a Volumetric Modulated Arc Therapy (VMAT) technique with millennium 120 (M120) multi-leaf collimators (MLC). Patients were immobilized with custom thermoplastic facemasks. The in-vivo transit portal images were measured with the EPID set at a source to detector distance (SSD) of 150 cm. The acquisition mode was set at portal dosimetry to facilitate non-synchronized image acquisition. The images were acquired and recorded at a rate of approximately 100 milliseconds per frame. The transit fluence was measured by an in-vivo portal dosimetry Watchdog system (WD)[26,29] on a daily basis. A script written in MATLAB (Mathworks, MA) was used to generate the integrated transit fluence from the cine images and exported into format readable by CONTOUR (MSKCC, NY) (Appendix II). CONTOUR was used to contour the ROI and calculate the $< \Delta\phi_{e,i} >$.

During the course of the treatment, a weekly cone beam computed tomography (CBCT) scan was acquired for each patient. A pair of kV-kV images was used on daily treatment setup. The residual daily setup variation is typically small but contributes to the uncertainty of the measurements. The CBCT was used to determine to volume change of the patient's

neck. The planning computed tomography (CT) and the corresponding planning structures were deformably registered to the CBCT scan. The deformed structures and the CBCT's were imported into a commercial treatment planning system (TPS). A structure, corresponding to the ROI, was created in the TPS for each CBCT spanning from condyloid process to C6 of the patient's spinal cord. The volumetric change ($\Delta V_{ROI,i}$) of the ROI of each CBCT was measured in the TPS as the standard measure of the volume change. The correlation and p-value between ΔV_{ROI} and the $< \Delta\phi_{e,i} >$ were analyzed to determine the statistical significance of the $< \Delta\phi_{e,i} >$. Linear regression between ΔV_{ROI} and the $< \Delta\phi_{e,i} >$ was also performed to determine the predictivity.

3.5 Phase 2: Clinical Study with Larger Group and Replanning point

An additional 15 patients were recruited for the test. Same analysis as described in 3.3 will be performed. A significant increase in grade 2 Xerostomia risk with a decrease of 10% or greater neck separation has been reported[20]. If the ROI is modeled as a combination half sphere of radius R representing the head, and a cylinder of radius r and height h representing the neck, then,

$$\frac{\Delta V_{ROI,i}}{V_{ROI}} = \frac{6\left(\frac{h}{r}\right)}{2\left(\frac{R}{r}\right)^3 + 3\left(\frac{h}{r}\right)} \frac{\Delta r}{r}$$

Using the typical dimensions of head and neck[82], a decrease of 10% neck separation corresponds to a decrease in $V_{ROI,i}$ between 5% to 8%. In this study, a threshold of 5.0% decrease in volume is used as the trigger for replanning. A set of replanning decisions

based on CBCT, assumed to follow binomial distribution, was obtained. The probability of replanning at session i, P_i, was modeled by using logistical regression with the transit fluence change and the CBCT based decision.

$$ln\left[\frac{P_i}{1-P_i}\right] = \beta_o + \beta_1 < \Delta\phi_{e,i} >$$

The *p*-values of the X^2, β_0 and β_1 coefficients were evaluated for the statistical significances of the logistic regression fit and the resulting coefficients. The association between the volumetric change and transit fluence change was assessed by the logarithmic odds ratio (OR). The reliability of the transit fluence signal in supporting the decision making of replanning was assessed by area under the curve (AUC) of the ROC curve.

3.6 Specificity Study with Salivary Glands Specific DSM

The three-dimensional salivary glands of each patient were contoured by a radiation oncologist in the planning CT. A set of angular dependent masks, $M_{sg}(\theta)$, based on the projections of the salivary glands onto the EPID at different gantry angles, θ, during treatments, was calculated. The value of each mask has the value of 1 inside the mask and 0 everywhere else. At any gantry, the salivary gland specific DSM, $\phi_e|_{sg}(\theta)$, is

$$\phi_e(\theta)|_{sg} = M_{sg}(\theta) \cdot \phi_e(\theta)$$

An organ specific ROI of the salivary gland, ROI_{sg}, defined as the sum of $M_{sg}(\theta)$ of angles spanned by a treatment, and the corresponding transit fluence, $\phi_e|_{sg,}$ were computed by integrating the $\phi_e(\theta)|_{sg}$ (Figure 5).

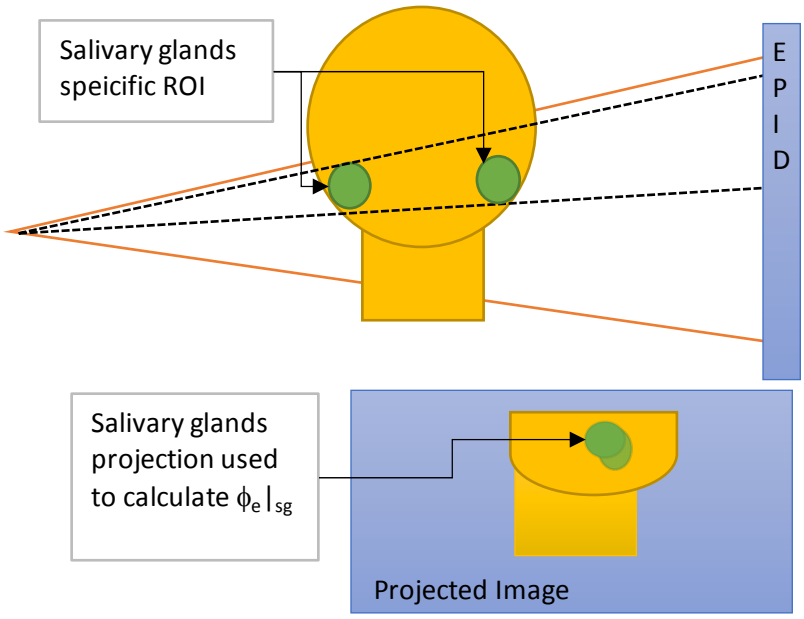

Figure 5: The schematic of projection of the salivary glands onto the EPID plane

The $< \Delta\phi_{e,i} >$ based on ROI_{sg}, $< \Delta\phi_{e,i} >|_{sg}$, will be calculated with the measured fluence in 3.5. The correlation and p-value between $\Delta V_{ROI,i}$ and the $< \Delta\phi_{e,i} >|_{sg}$ were analyzed to determine the statistical significance of the $< \Delta\phi_{e,i} >|_{sg}$. The correlation and p-value were compared with those from $< \Delta\phi_{e,i} >$ to ascertain the specificity improvement.

3.7 Xerostomia and Mucositis Risk Association

The MSKCC patient QoL questionnaire, which is based on MDADI, was used in this study (Figure 6). Each set of questions was sub-divided into four subsets[61] and graded according to MDADI protocol: global, emotion, physical and functional. Table 1 shows the questions belonging to the four subsets. The score of each subset is defined as the sum of the scores of the questions in the corresponding subset. The total MDADI score is the

sum of all the subset question scores. The likelihood of post treatment xerostomia and mucositis is defined as the decrease in the post-treatment MDADI score. A lower post-treatment MDADI score means a decrease of salivary function and higher risk of xerostomia.

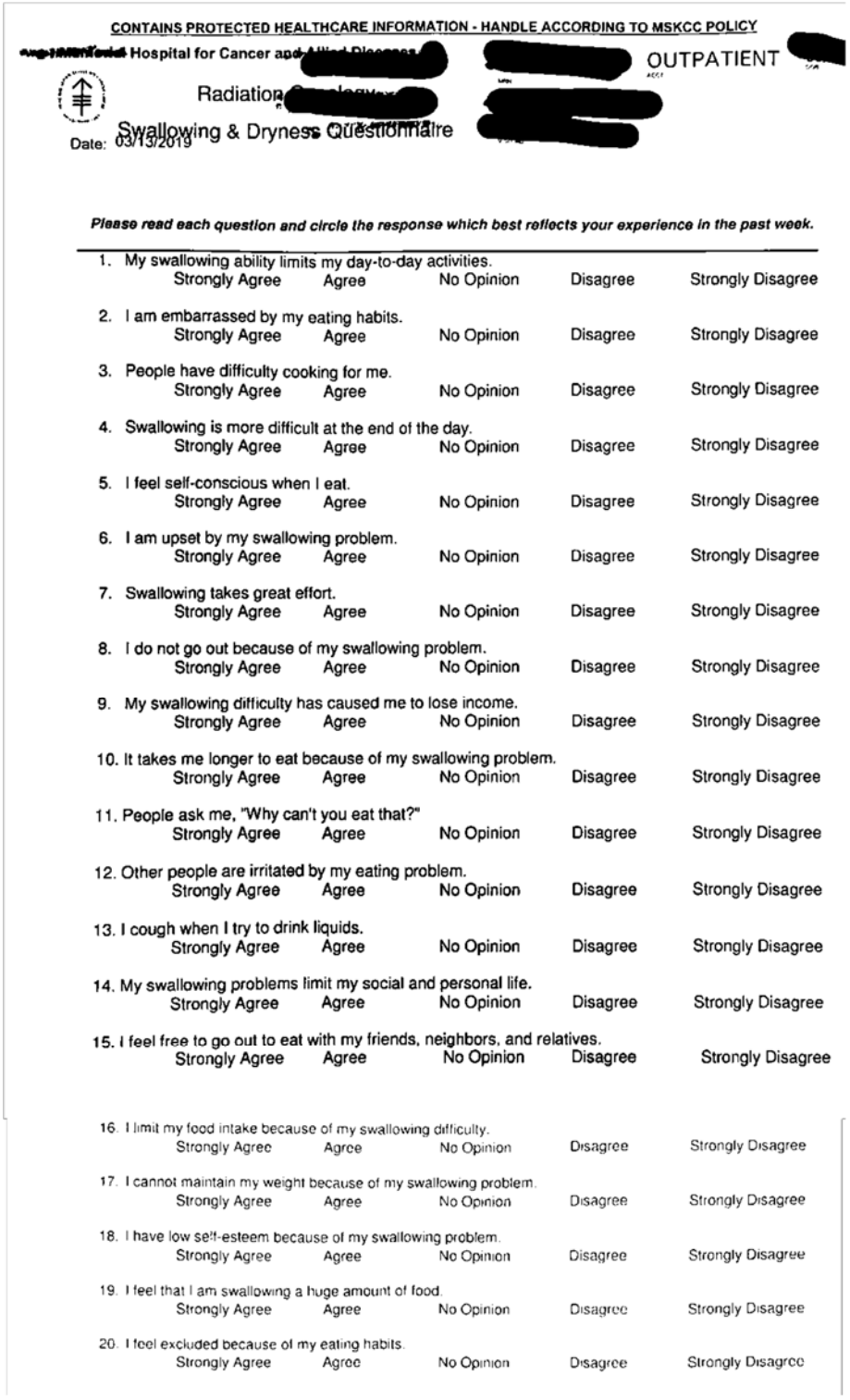

CONTAINS PROTECTED HEALTHCARE INFORMATION - HANDLE ACCORDING TO MSKCC POLICY

[redacted] Hospital for Cancer and [redacted] OUTPATIENT [redacted]

Radiation [redacted]

Date: 03/13/2019 Swallowing & Dryness Questionnaire [redacted]

Please read each question and circle the response which best reflects your experience in the past week.

1. My swallowing ability limits my day-to-day activities.
   Strongly Agree Agree No Opinion Disagree Strongly Disagree
2. I am embarrassed by my eating habits.
   Strongly Agree Agree No Opinion Disagree Strongly Disagree
3. People have difficulty cooking for me.
   Strongly Agree Agree No Opinion Disagree Strongly Disagree
4. Swallowing is more difficult at the end of the day.
   Strongly Agree Agree No Opinion Disagree Strongly Disagree
5. I feel self-conscious when I eat.
   Strongly Agree Agree No Opinion Disagree Strongly Disagree
6. I am upset by my swallowing problem.
   Strongly Agree Agree No Opinion Disagree Strongly Disagree
7. Swallowing takes great effort.
   Strongly Agree Agree No Opinion Disagree Strongly Disagree
8. I do not go out because of my swallowing problem.
   Strongly Agree Agree No Opinion Disagree Strongly Disagree
9. My swallowing difficulty has caused me to lose income.
   Strongly Agree Agree No Opinion Disagree Strongly Disagree
10. It takes me longer to eat because of my swallowing problem.
    Strongly Agree Agree No Opinion Disagree Strongly Disagree
11. People ask me, "Why can't you eat that?"
    Strongly Agree Agree No Opinion Disagree Strongly Disagree
12. Other people are irritated by my eating problem.
    Strongly Agree Agree No Opinion Disagree Strongly Disagree
13. I cough when I try to drink liquids.
    Strongly Agree Agree No Opinion Disagree Strongly Disagree
14. My swallowing problems limit my social and personal life.
    Strongly Agree Agree No Opinion Disagree Strongly Disagree
15. I feel free to go out to eat with my friends, neighbors, and relatives.
    Strongly Agree Agree No Opinion Disagree Strongly Disagree
16. I limit my food intake because of my swallowing difficulty.
    Strongly Agree Agree No Opinion Disagree Strongly Disagree
17. I cannot maintain my weight because of my swallowing problem.
    Strongly Agree Agree No Opinion Disagree Strongly Disagree
18. I have low self-esteem because of my swallowing problem.
    Strongly Agree Agree No Opinion Disagree Strongly Disagree
19. I feel that I am swallowing a huge amount of food.
    Strongly Agree Agree No Opinion Disagree Strongly Disagree
20. I feel excluded because of my eating habits.
    Strongly Agree Agree No Opinion Disagree Strongly Disagree

Figure 6: MSK QoL that is based on MDADI

Table 1:The four sebsets of MDADI and the corresponding question number.

Subsets of MDADI	Question number
Global	1
Emotion	2, 5, 6, 8, 12, 18
Functional	3, 9, 14, 15, 20
Physical	4, 7, 10, 11, 13, 16, 17, 19

The association of between each of the four subsets of MDADI and each relevant factor were analyzed using ranked Pearson correlation. These factors are age, gender, mean dose to salivary glands, weight change, $\Delta V_{ROI,i}$, $< \Delta\phi_{e,i} >$, and $< \Delta\phi_{e,i} >|_{sg}$. Here male and female were denoted as "1" and "0" for analysis purpose. The p-value of the ranked Pearson correlation factors, ρ, were used to assess the significance of the association. The p-value less 0.05 and 0.10 were used for the thresholds for the classification of the statistically significant and clinically important association[83] respectively. 95% confidence intervals, 95% CI, were also calculated. The statistical power[83] of the statistically significant factors were also calculated.

Chapter 4

Results

4.1 Phantom Study

Figure 7(a) shows the measured transit fluence distributions of the phantom with and without the 5mm bolus. Figure 7(b) shows the difference, $\Delta\phi$, between the two fluence distributions. With the reduction in tissue, an overall increase in fluence was observed.

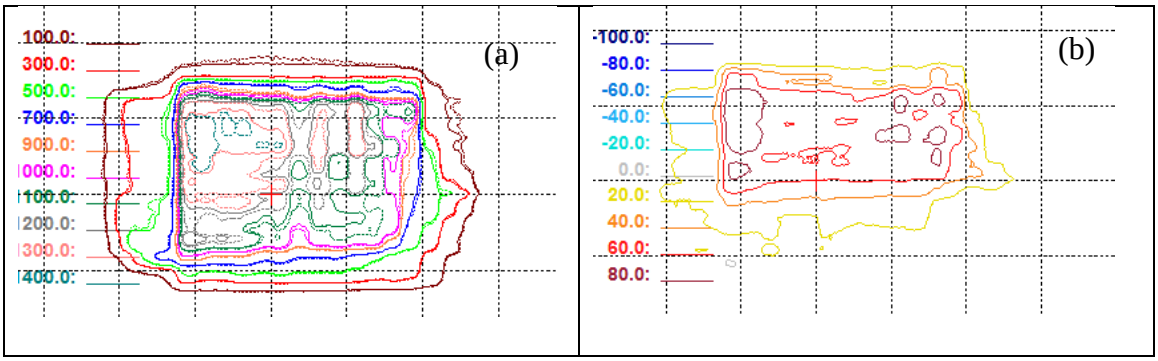

Figure 7 (a) shows the overlay of transit fluence with 5mm bolus (solid line) and no bolus (dotted lines); (b) shows the difference of the two fluences

The $< \Delta\phi_e >$ was found to be +6.0% as a result of a decrease in 1cm radiological pathlength.

4.2 Phase 1 Clinical Study

Five patients were recruited in a small clinical study. Figure 8 shows an example of the variation in measured ΔV_{ROI} and $< \Delta\phi_{e,i} >$ for a single patient as a function of treatment day. The volume change by treatment day 15 for this patient was 6.8%. Figure 8 shows the relationship between ΔV_{ROI} and $< \Delta\phi_{e,i} >$ of the five patients. The correlation ΔV_{ROI}

and $< \Delta\phi_e >$ was found to be -0.896 with the p-value less than 0.001. The R^2 of the linear regression between ΔV_{ROI} and $< \Delta\phi_{e,i} >$ is 0.803 with a slope of the regression of -1.33. This indicates a statistically significant correlation between the exit fluence change and the corresponding volumetric change.

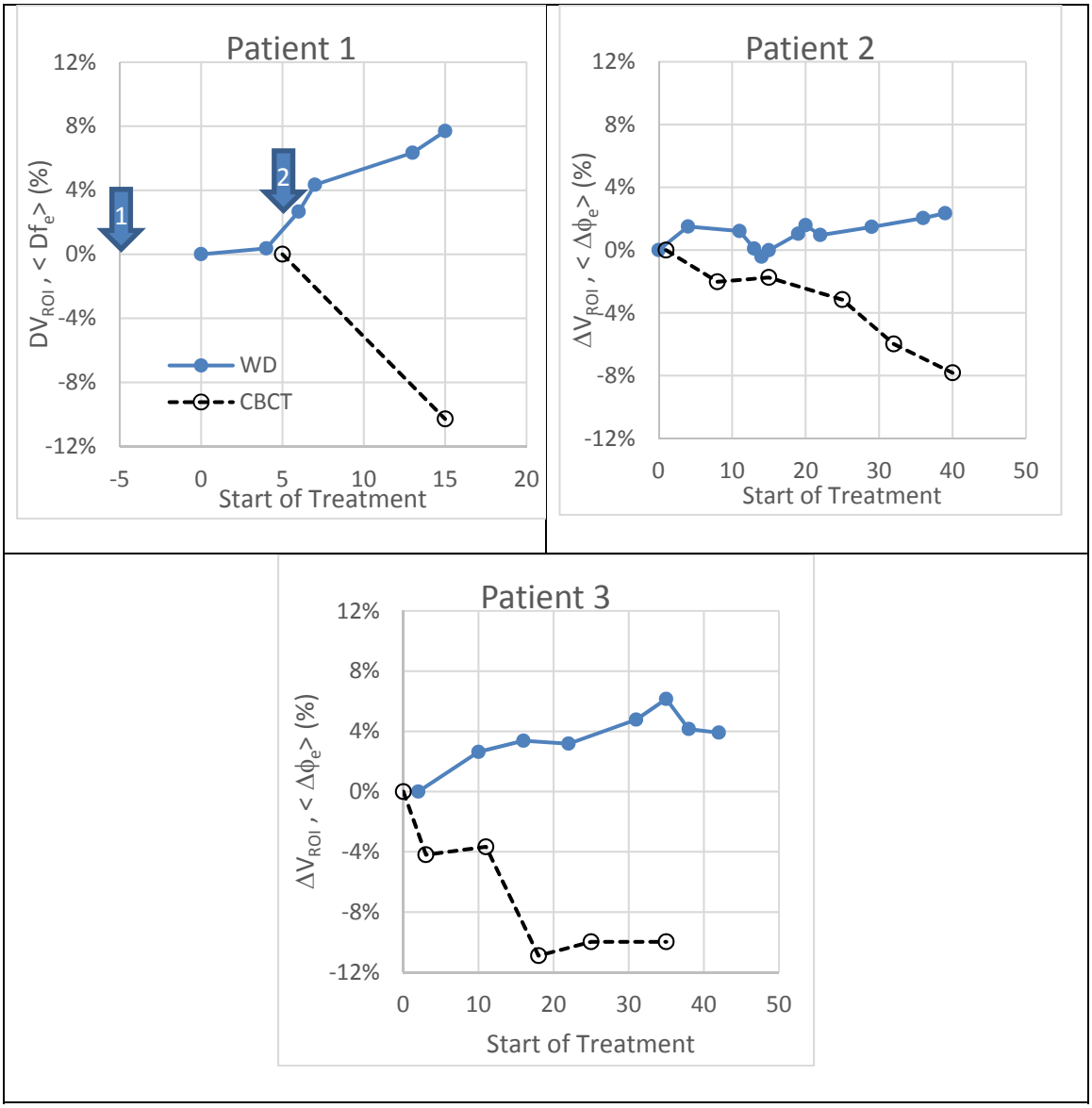

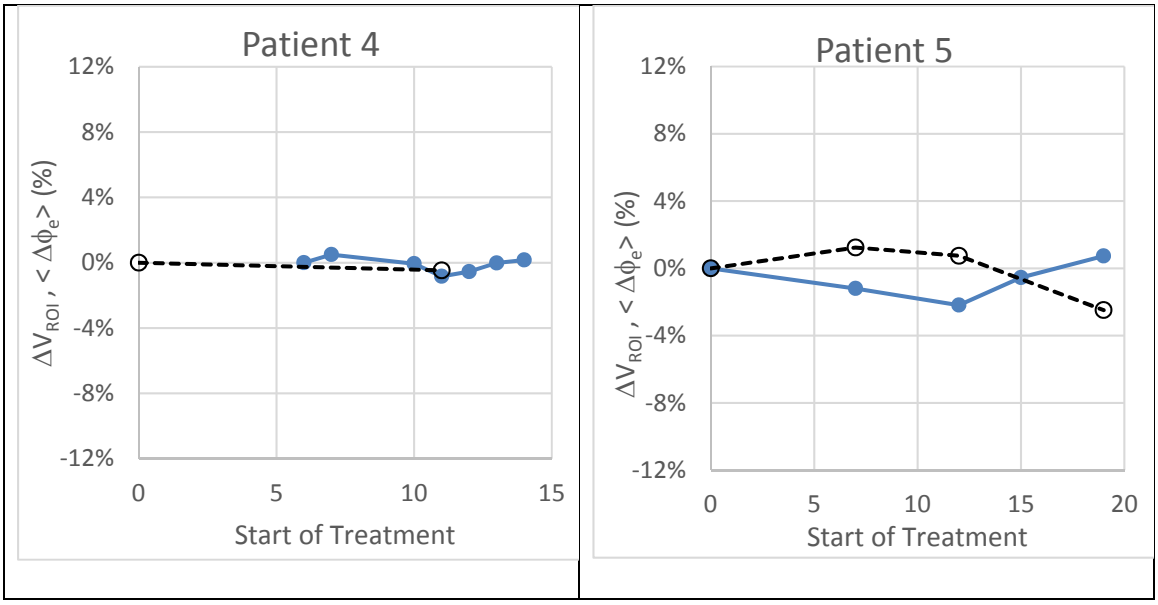

Figure 8: The fluence change $< \phi_{e,i} >$ and volumetric change (ΔV_{ROI}). Results measured from ϕ_e (solid *line) and CBCT (dotted line) respectively*

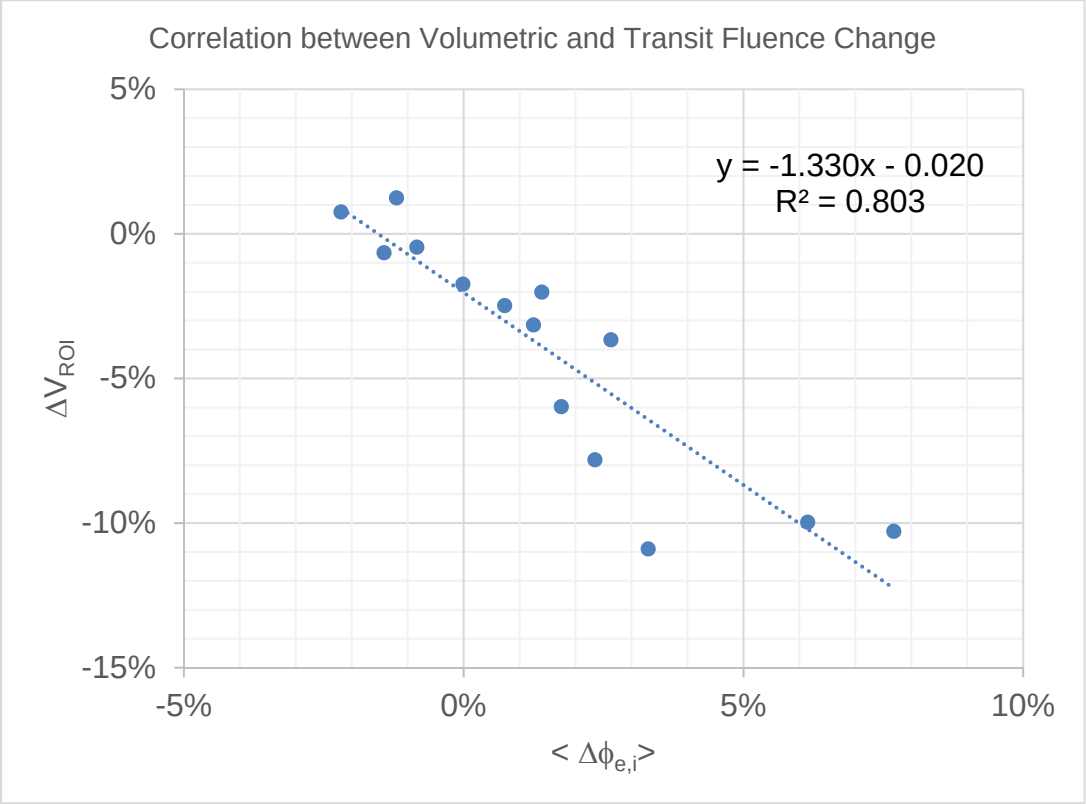

Figure 9: Phase 1 correlation study between ΔV_{ROI} and $<\Delta\phi_{e,i}>$ based on five patients

4.3 Phase 2 Clinical Study

An additional nineteen patients were recruited in this study and brought the total number to twenty-four. Nine of the twenty-four patients exhibited larger than 5.0% volumetric reduction during their treatment courses. Figure 10a shows the $\Delta V_{ROI,i}$ and $<\Delta\phi_{e,i}>$ variation of patients with more than 5.0% volumetric decrease. The maximum ΔV_{ROI} ranges between -10.9% and 11.3% corresponds to a change of $<\Delta\phi_{e,i}>$ between 3.9% to -6.2%. The time observed for the volume to decrease 5.0% or more ranges from 10 to 29 days. For patients with a maximum decrease in $\Delta V_{ROI,i}$ less than -5.0%, the change

in transit fluence was correspondingly smaller, with all $< \Delta\phi_{e,i} >$ values, being less than 3.5%. (Figure 10b)

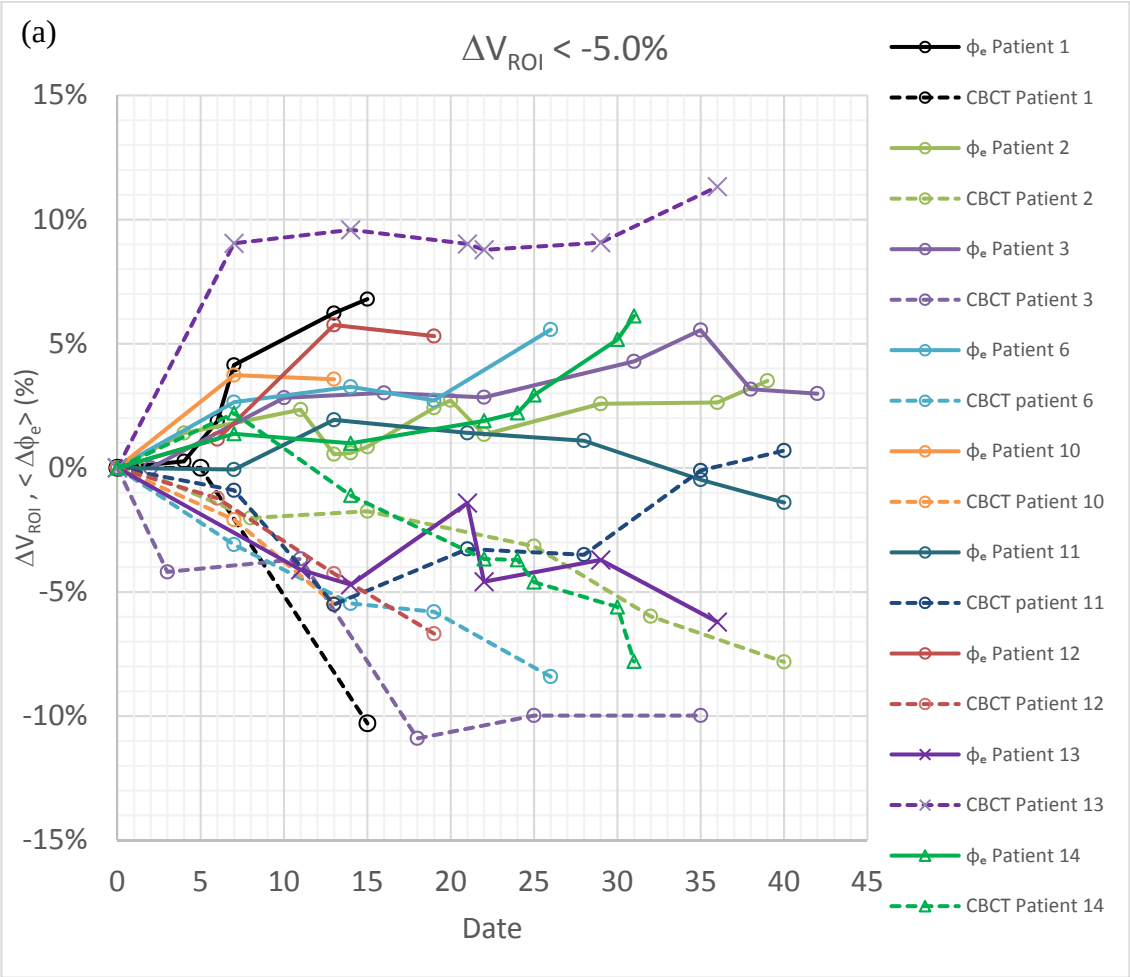

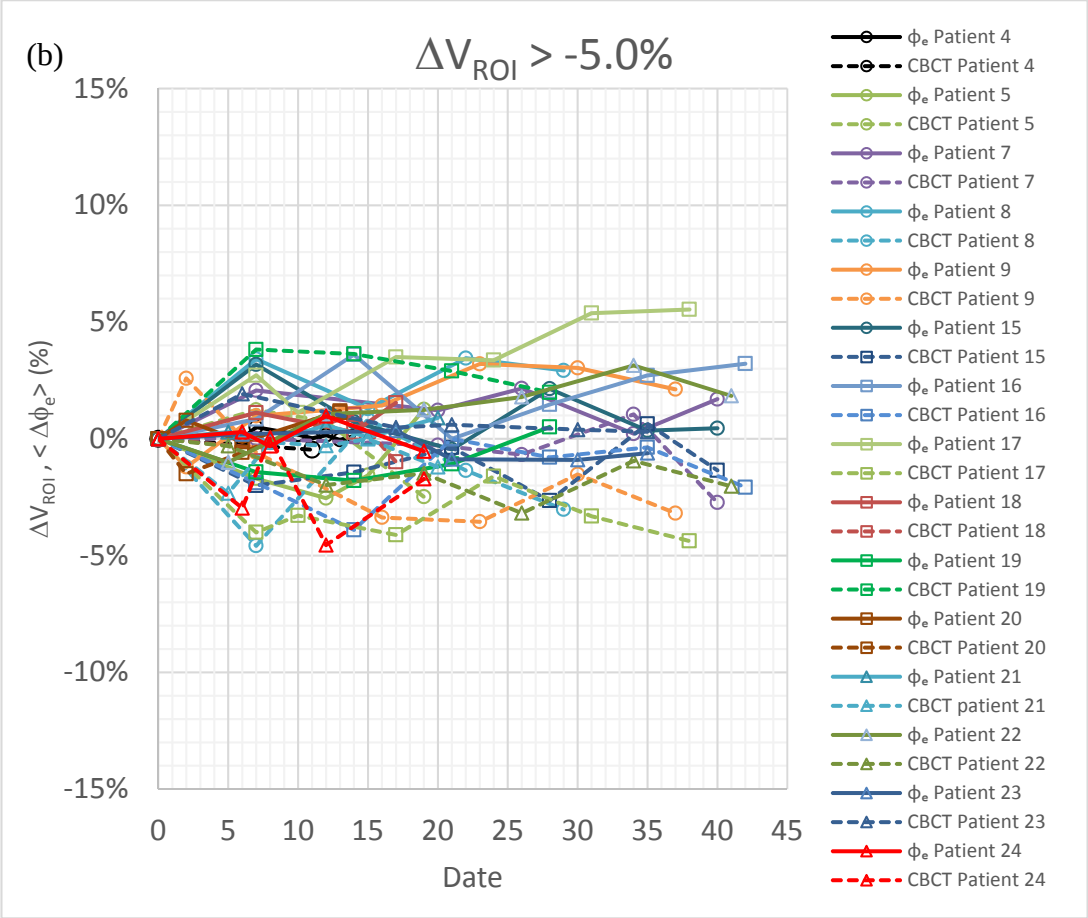

Figure 10: The variation of transit fluence change and volumetric change of patients at different treatment days. (a) patients with volume reduction of more than 5%; (b) patients with volume reduction less than 5%.

Excluding the baseline points, a total of 110 pairs of ΔV_{ROI} and $< \Delta\phi_{e,i} >$ were obtained. The correlation was found to be -0.84 with the p-value less than 0.001.

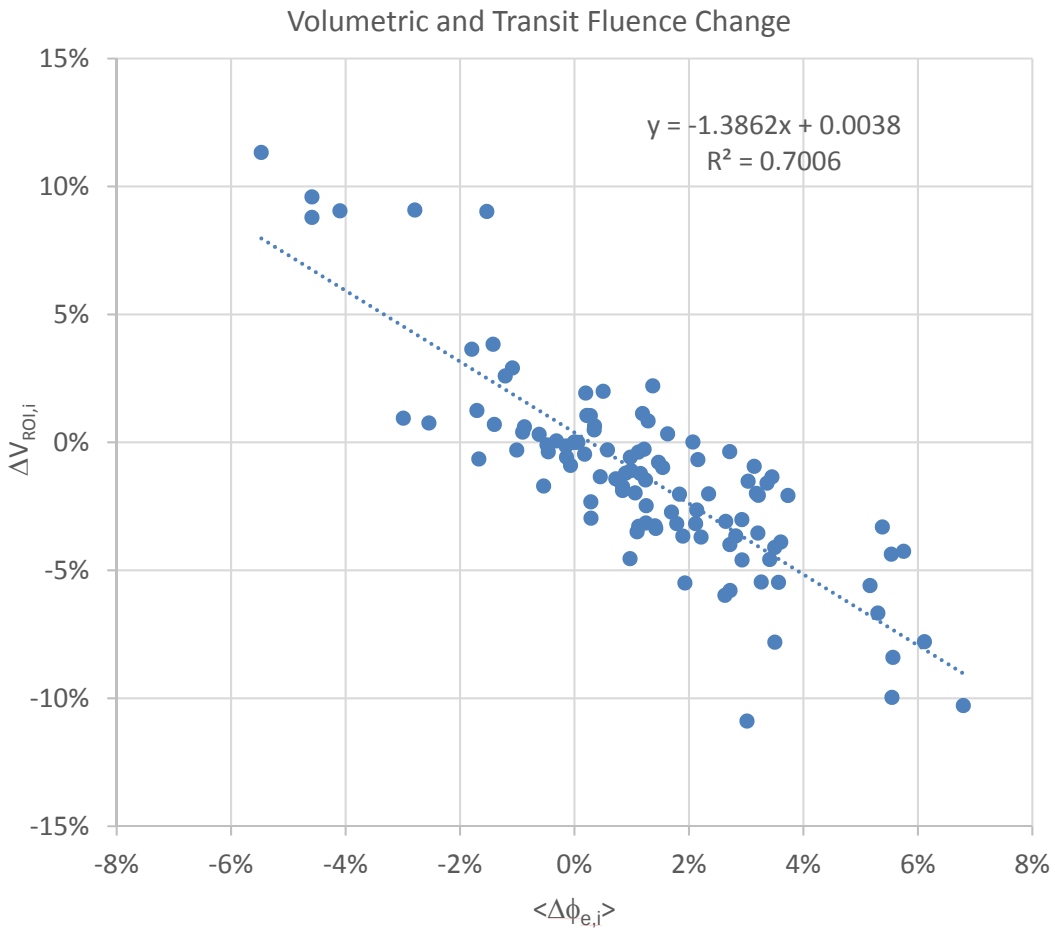

Figure 11: Scatter plot of the transit fluence variation and CBCT volumetric changes of the ten patients to assess the correlation between fluence and volume change during the course of treatment.

Figure 11 shows the scatter plot of ΔV_{ROI} and $< \Delta\phi_{e,i}>$. The R^2 of the linear regression between ΔV_{ROI} and $< \Delta\phi_{e,i}>$ is 0.70 with a slope of the regression of -1.39. The X^2 statistic of the model is 17.4 with a p-value less than 0.001. The β_0 and β_1 of the logistic regression are -6.84 and 87.0 respectively. The corresponding p-values are 0.001 and 0.003 indicating both factors are statistically significant. The OR of $< \Delta\phi_{e,i}>$ was found to be 87.04 with the 95% confident interval of [27.4, 146.6]. The AUC of the ROC (Figure 12) is 0.91.

This indicates a statistically significant association between the transit fluence change and the corresponding volumetric change based replanning trigger.

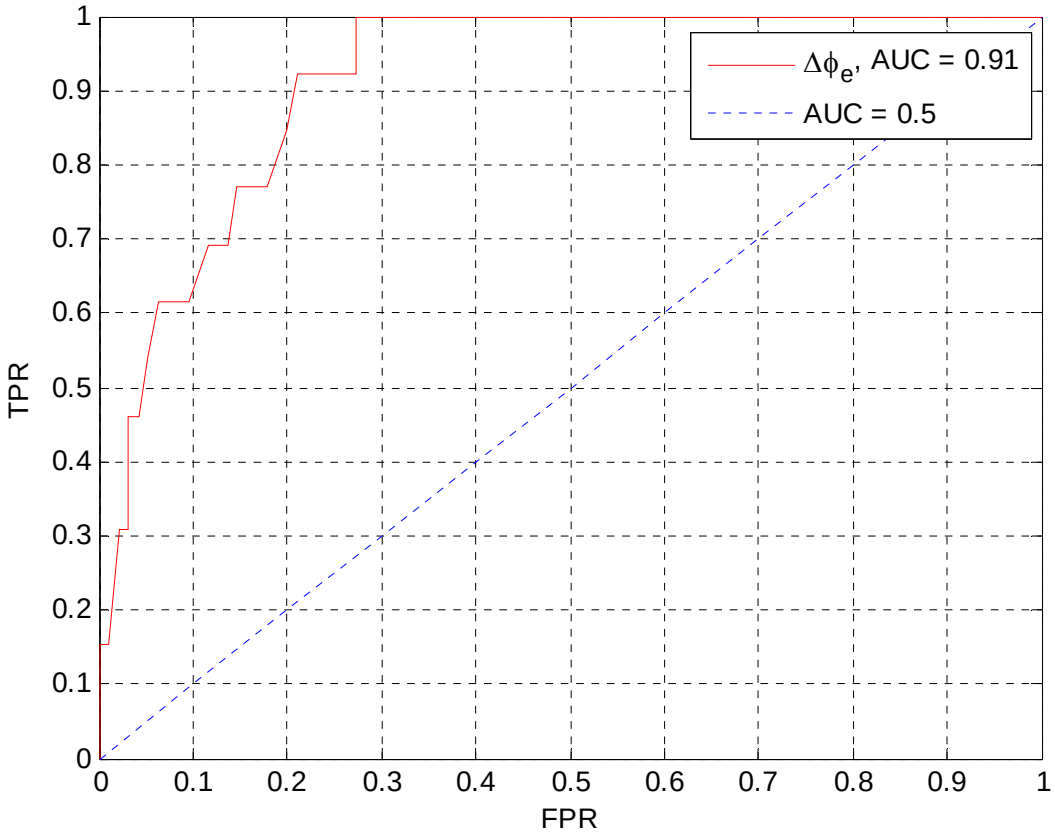

Figure 12: The ROC of the logistical regression model of the WD signal based on ten patients and a replanning threshold of 5% volume reduction corresponding to an increase risk of grade 2 Xerostomia.

4.4 Salivary Gland Specific DSM

The correlation between $< \Delta\phi_{e,i} >$ and $< \Delta\phi_{e,i} > |_{sg}$ of the 24 patients were calculated and found to be 0.776 with p-value < 0.001 (Figure 13). Significant association was found between masked and non-masked cases (Figure 13). The correlation between $< \Delta\phi_{e,i} > |_{sg}$ and ΔV_{ROI} was found to be -0.62 with p-value < 0.001 (Figure 14). The result indicates an association between masked transit fluence and the volumetric change.

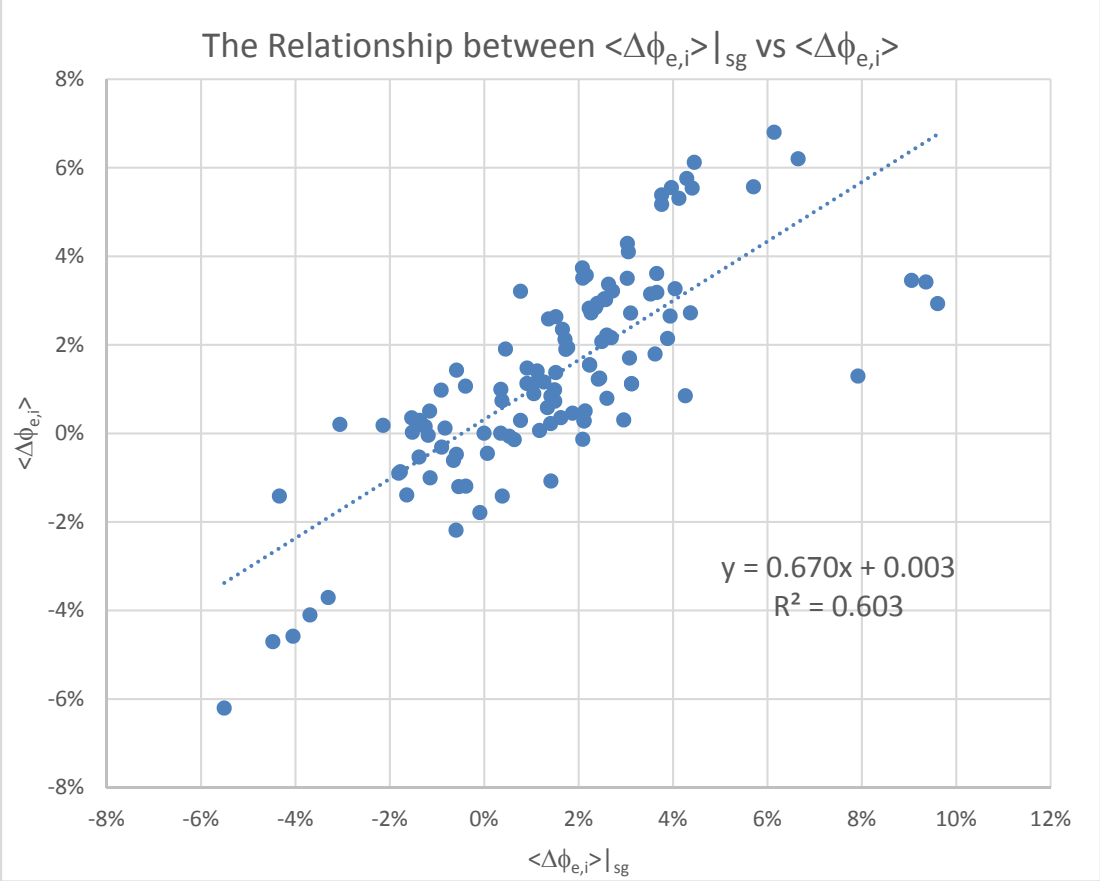

Figure 13: The correlation between $< \Delta\phi_{e,i} >$ and $< \Delta\phi_{e,i} > |_{sg}$ of 24 patients

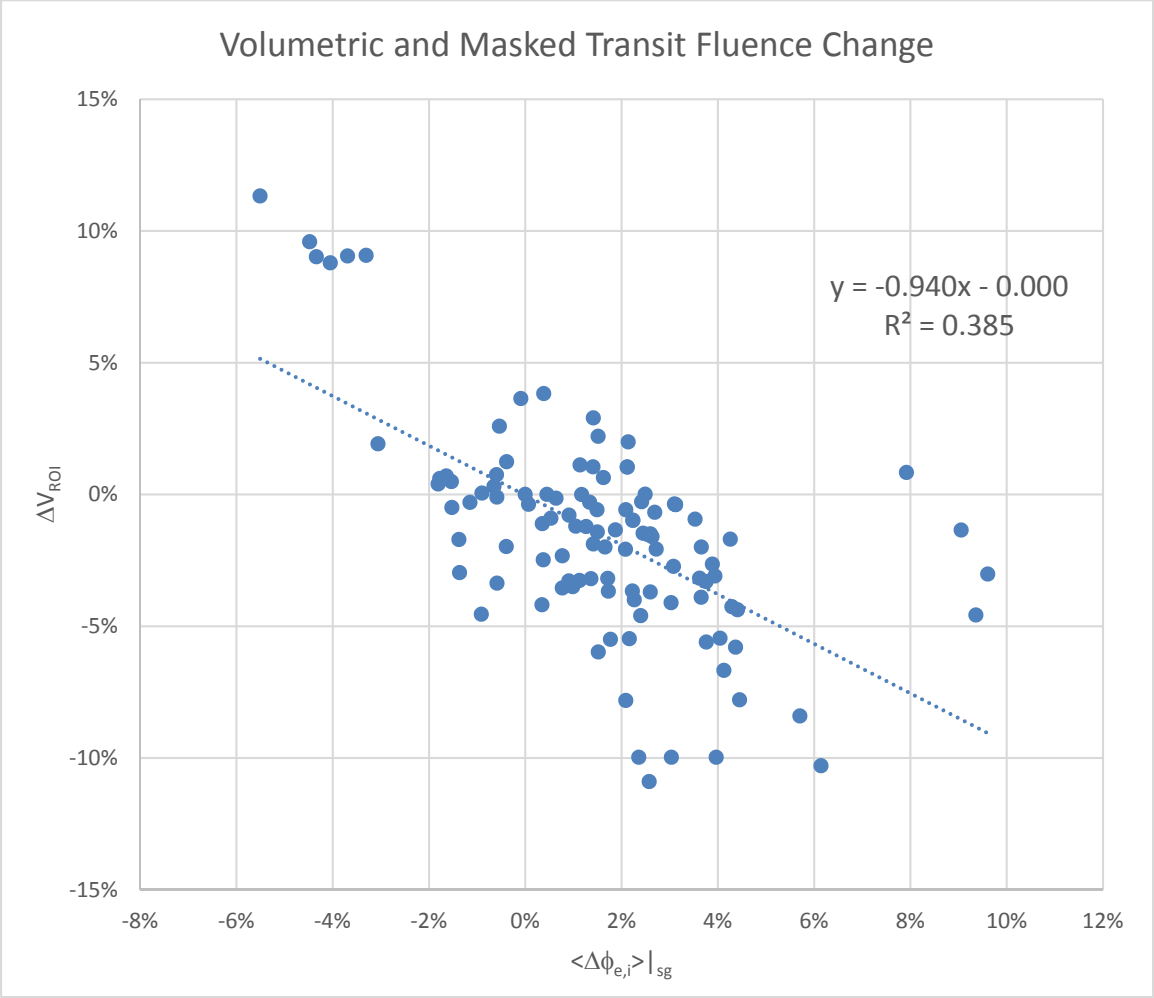

Figure 14: The scatter plot between $< \Delta\phi_{e,i} >|_{sg}$ and ΔV_{ROI} of 24 patients

4.5 Xerostomia Risk Association

Twenty-one of the twenty-four patients in this study answered the questionnaire. The average age was found to be 62.7 years old. The gender mix was found to be 29% female and 71% male. The age and gender distribution of all the patients were summarized in Table 2. Table 3 shows the change in MDADI scores in the four subsets and the total after the radiation treatment. The ranked values of the QoL change are shown in Table 4.

Table 2: Demography of the 21 patients

Age	Average	62.7
	Maximum	86.0
	Minimum	32.0
	Standard deviation	11.6
Gender	Female	6 (29%)
	Male	15 (71%)
	Total	21

Table 3: The change of MDADI of twenty-one patients after radiation treatment

Global	Emotion	Physical	Functional	Total
-1	8	-10	-2	-5
-3	15	-16	-5	-9
0	12	-7	-9	-4
1	-6	-1	2	-4
-2	6	-4	-2	-2
-1	6	-3	-5	-3
0	0	0	0	0
-1	9	-9	-9	-10
-1	12	-5	-4	2
0	8	-7	1	2
-2	8	-9	-3	-6
1	11	-2	-6	4
0	0	-8	-8	-16
0	0	0	4	4
0	1	3	1	5
-1	6	-10	-3	-8
-3	9	-9	-3	-6
0	0	1	0	1
0	4	-12	-6	-14
-1	3	-7	-3	-8
0	-2	-2	1	-3

Table 4: The ranked values of the QoL change of the twenty-one patients

Global	Emotion	Physical	Functional	Total
14.5	8.0	18.5	8.5	13.0
20.5	1.0	21.0	15.5	18.0
7.0	2.5	12.0	20.5	11.5
1.5	21.0	5.0	2.0	11.5
18.5	11.0	9.0	8.5	8.0
14.5	11.0	8.0	15.5	9.5
7.0	17.5	3.5	6.5	7.0
14.5	5.5	16.0	20.5	19.0
14.5	2.5	10.0	14.0	4.5
7.0	8.0	12.0	4.0	4.5
18.5	8.0	16.0	11.5	14.5
1.5	4.0	6.5	17.5	2.5
7.0	17.5	14.0	19.0	21.0
7.0	17.5	3.5	1.0	2.5
7.0	15.0	1.0	4.0	1.0
14.5	11.0	18.5	11.5	16.5
20.5	5.5	16.0	11.5	14.5
7.0	17.5	2.0	6.5	6.0
7.0	13.0	20.0	17.5	20.0
14.5	14.0	12.0	11.5	16.5
7.0	20.0	6.5	4.0	9.5

4.5.1 Age

The scatter plot of patient age with the change of MDADI subset and total scores are shown in Figure 15a and b respectively. The ranked MDADI scores and age of the patients are shown in Table 12 in Appendix IV. The rank correlation coefficients of age for global, emotion, physical, functional and total were found to be 0.22, 0.14, 0.08, -0.08 and 0.30 respectively (Table 5). All p-values were found to be larger than 0.1 implying age is not significantly associated with MDADI.

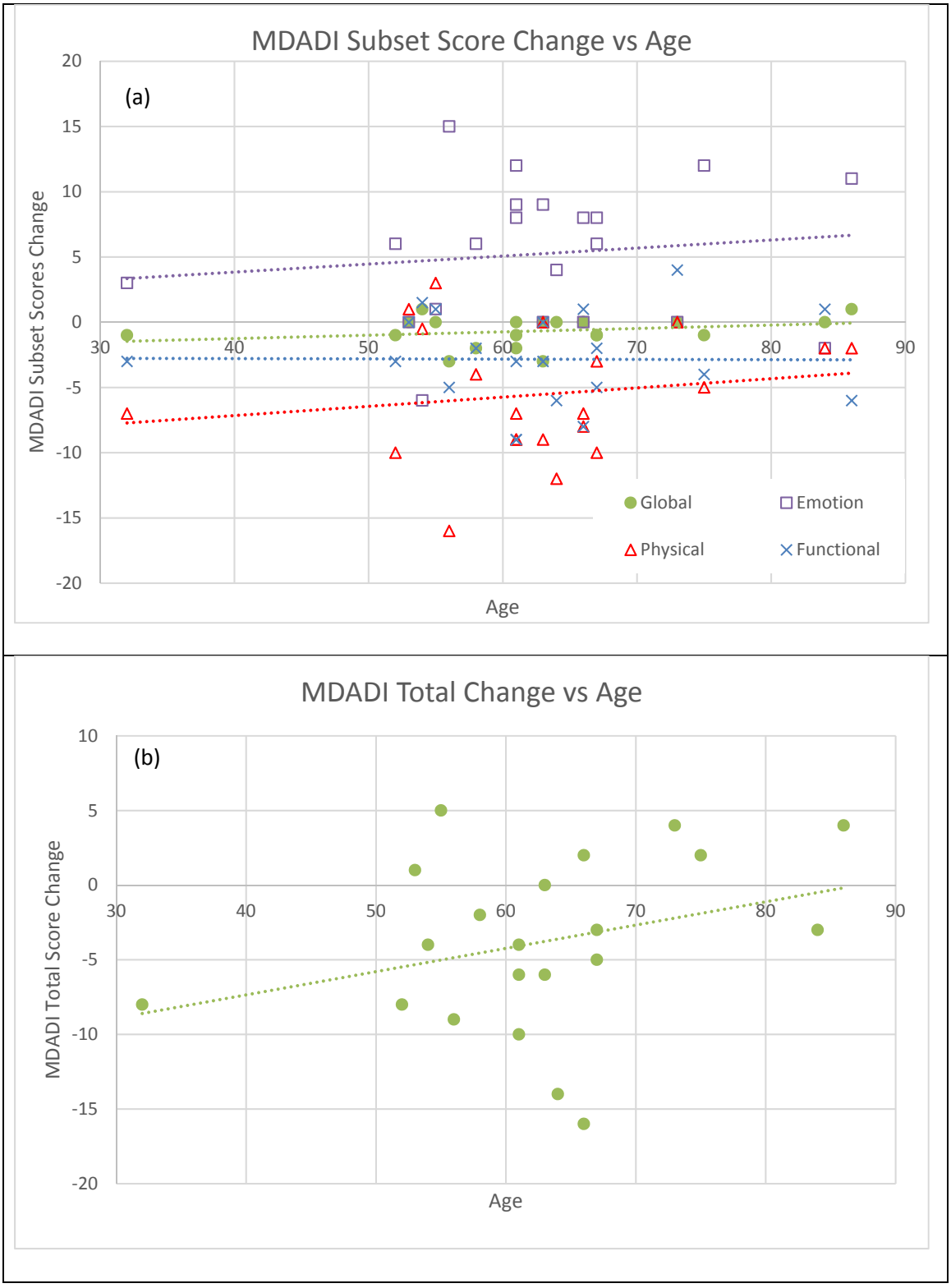

Figure 15: The relationship of patient age with the MDADI change (a) subsets and (b) total.

Table 5: Spearman rank correlation between MADI subset scores and age

Age	spearman rank correlation				
	Global	Emotion	Physical	Functional	Total
ρ	0.22	0.14	0.08	-0.08	0.30
95% CI	0.68	0.60	0.54	0.38	0.76
	-0.24	-0.33	-0.39	-0.54	-0.16
p-value	0.334	0.559	0.744	0.729	0.182

4.5.2 Gender

Figure 16a shows the MDADI subset change with patient gender. The change of the total scores with gender is shown in Figure 16b. The ranked MDADI and gender were calculated and shown in Table 13 in Appendix IV. The rank correlation of gender with global, emotion, physical, functional and total MDADI scores were found to be -0.30, -0.23, 0.12, 0.17 and 0.09 respectively (Table 6). All the p-values were found to be larger than 0.1. This implies the associations are not statistically significant.

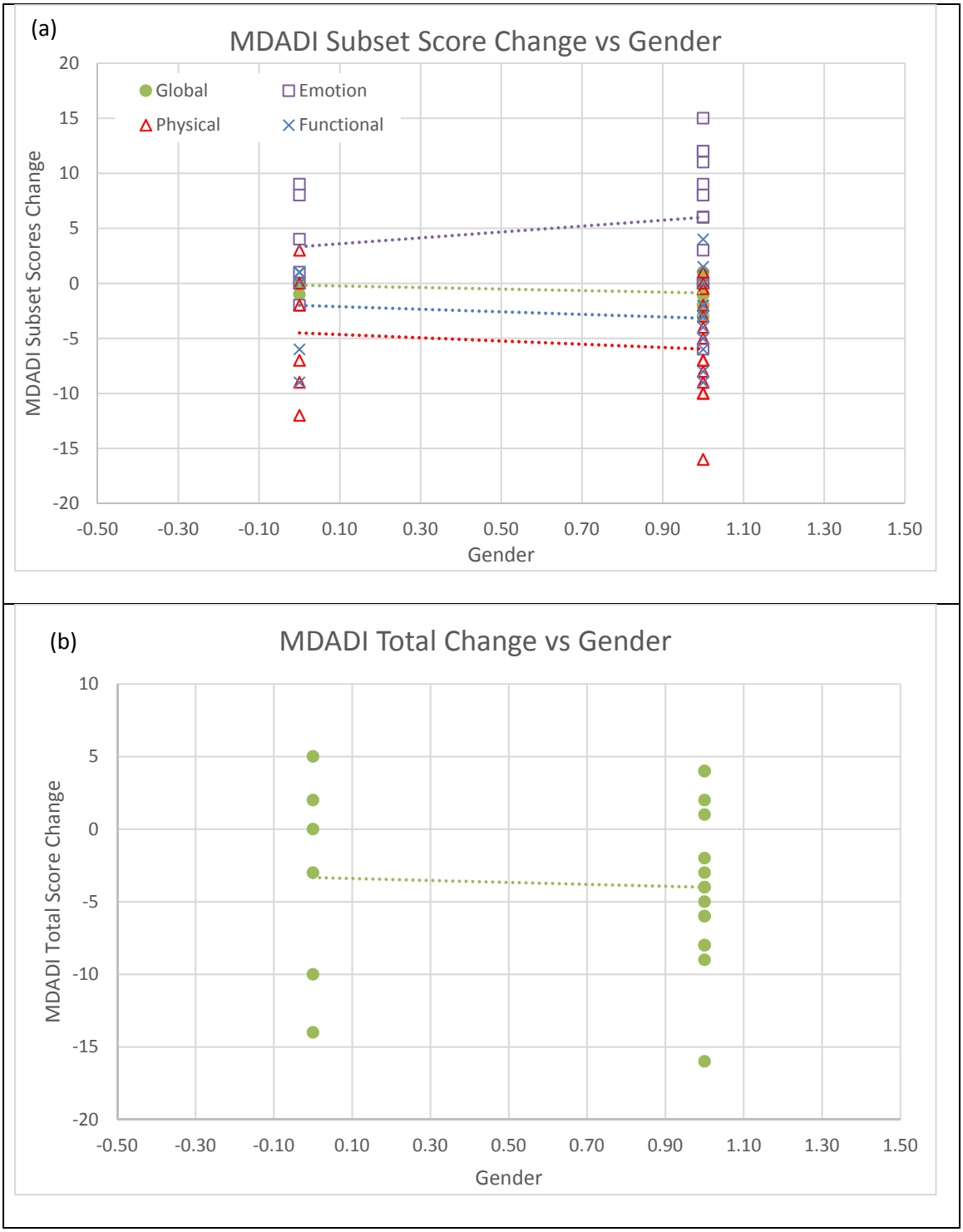

Figure 16: The relationship of patient gender with the MDADI change (a) subsets and (b) total.

Table 6: Rank Pearson correlation of MDADI scores and gender of the patients

Gender	spearman rank correlation				
	Global	Emotion	Physical	Functional	Total
ρ	-0.30	-0.23	0.12	0.17	0.09
95% CI	0.16	0.23	0.58	0.63	0.55
	-0.77	-0.69	-0.34	-0.30	-0.37
p-value	0.182	0.321	0.597	0.471	0.707

4.5.3 Mean Dose to the Salivary Glands $<D_{sg}>$

The relationship between $<D_{sg}>$ and MDADI subsets change were plotted in Figure 17a. The relationship between $<D_{sg}>$ and MDADI total change was plotted in Figure 17b. The ranked MDADI and $<D_{sg}>$ were calculated and shown in Table 14 in Appendix IV. The Spearman rank correlation coefficient of $<D_{sg}>$ with global, emotion, physical, functional and total were found to be -0.04, 0.28, -0.21, -0.39, and -0.13. respectively (Table 7). The p-values of functional subset was found to be 0.081 and the remaining scores were found to be higher than 0.10. This implies $<D_{sg}>$, except functional subset, is not significantly correlated with MDADI. For the functional subset, however, $<D_{sg}>$ was found to have a trend of association with possible clinical importance.

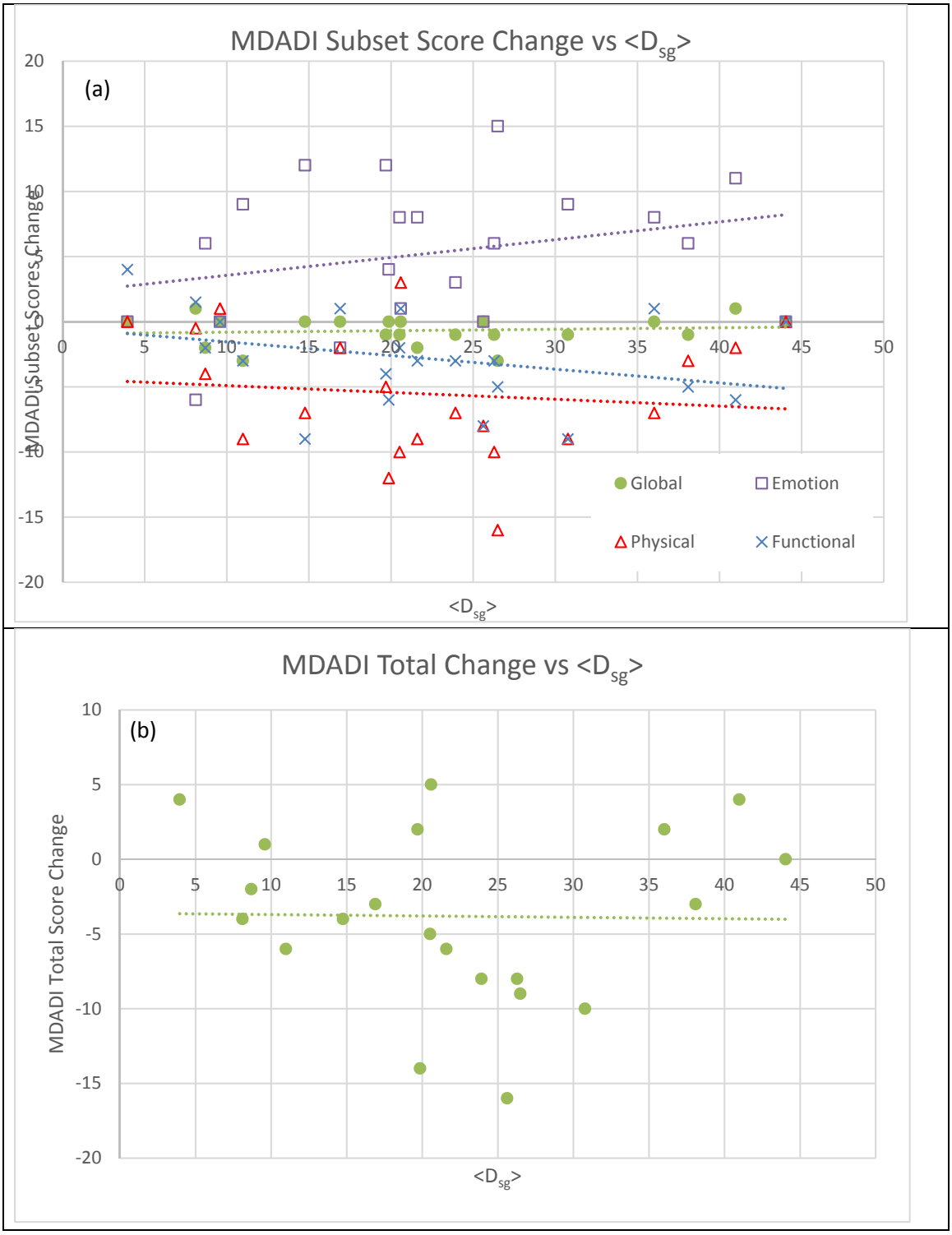

Figure 17: The relationship of <D_{sg}> with the MDADI change (a) subsets and (b) total.

Table 7: Rank Pearson correlation of MDADI scores and <D_{sg}>

<$Dose_{SG}$>	spearman rank correlation				
	Global	Emotion	Physical	Functional	Total
ρ	-0.04	0.28	-0.21	-0.39	-0.13
95% CI	0.43	0.74	0.25	0.07	0.34
	-0.50	-0.18	-0.67	-0.85	-0.59
p-value	0.878	0.215	0.358	0.081	0.586

4.5.4 Weight Change

Figure 18a and b show the scatter plot of weight change of the patients and MDADI subset and total score change respectively. The ranked weight change, Δweight, was calculated and shown in Table 15 in Appendix IV. All p-values of the ranked correlation were found to be larger than 0.1 (Table 8). This implies the relationship between weight change and all the MDADI scores are not significant.

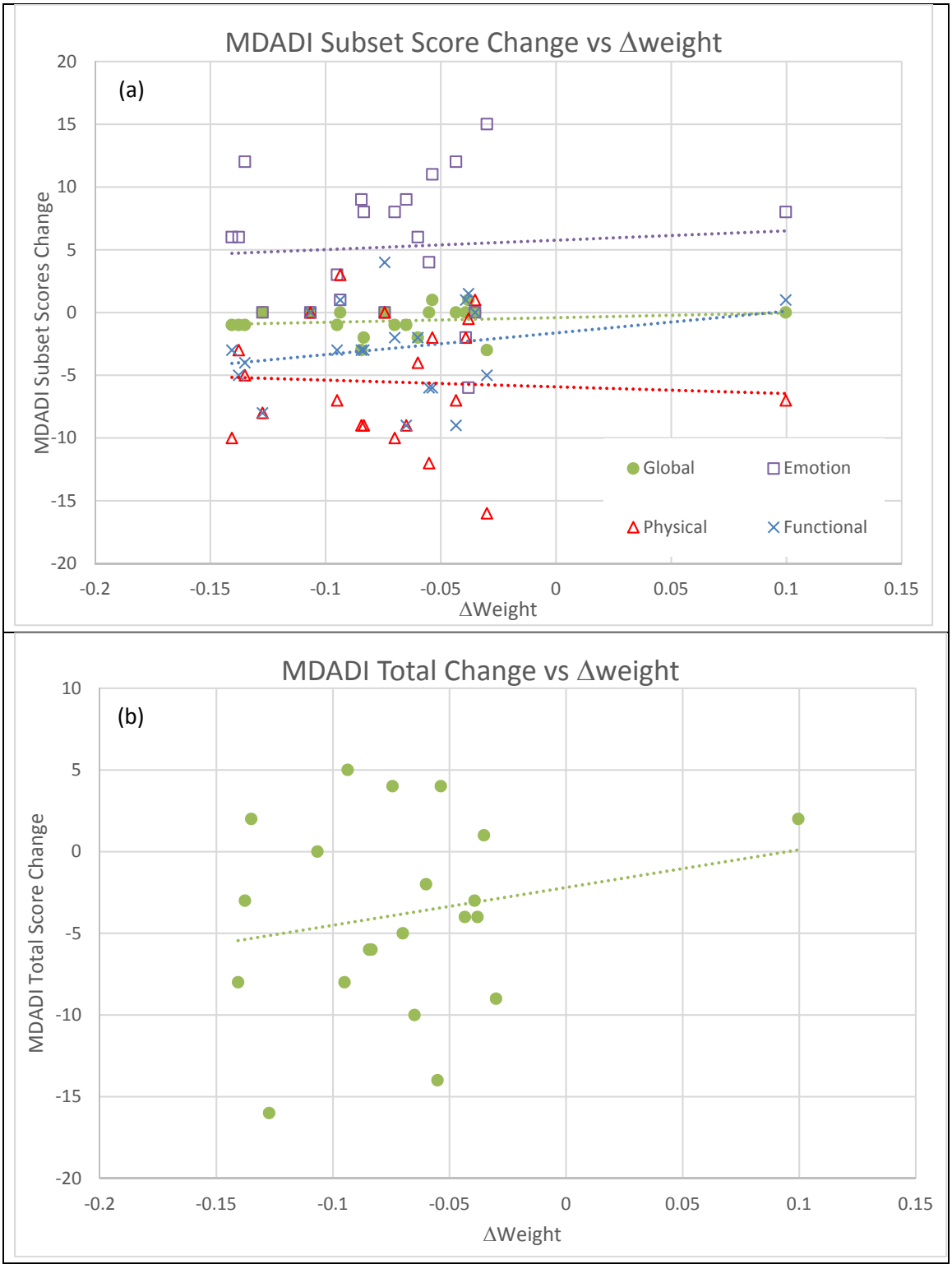

Figure 18: The relationship of ∆weight with the MDADI change (a) subsets and (b) total.

Table 8: Rank Pearson correlation of MDADI scores and Δweight

Δweight	spearman rank correlation				
	Global	Emotion	Physical	Functional	Total
ρ	0.29	0.06	0.03	0.18	0.11
95% CI	0.75	0.52	0.49	0.64	0.57
	-0.17	-0.40	-0.43	-0.28	-0.36
p-value	0.201	0.798	0.891	0.432	0.645

4.5.5 Volumetric Change $\Delta V_{ROI,i}$

The volumetric change of patient, $\Delta V_{ROI,i}$, with MDADI subset and total scores are plotted in Figure 19a and b respectively. The ranked ΔV_{ROI} were calculated and tabulated in Table 16 in Appendix IV. The ranked correlation of $\Delta V_{ROI,i}$ with MDADI global, emotion, physical, and functional subsets were found to be 0.44, -0.34, 0.47 and 0.44 respectively (Table 9). The ranked correlation for MDADI total score was found to be 0.40. Three of the four subsets, global, physical and functional, were found to be statistically significant correlation with $\Delta V_{ROI,i}$. The statistical power of the correlation with the global, physical and functional subsets were found to be 0.5, 0.6 and 0.5 respectively. The MDADI total was also found to have a relational trend with volumetric change with possible clinically importance (p-value = 0.073).

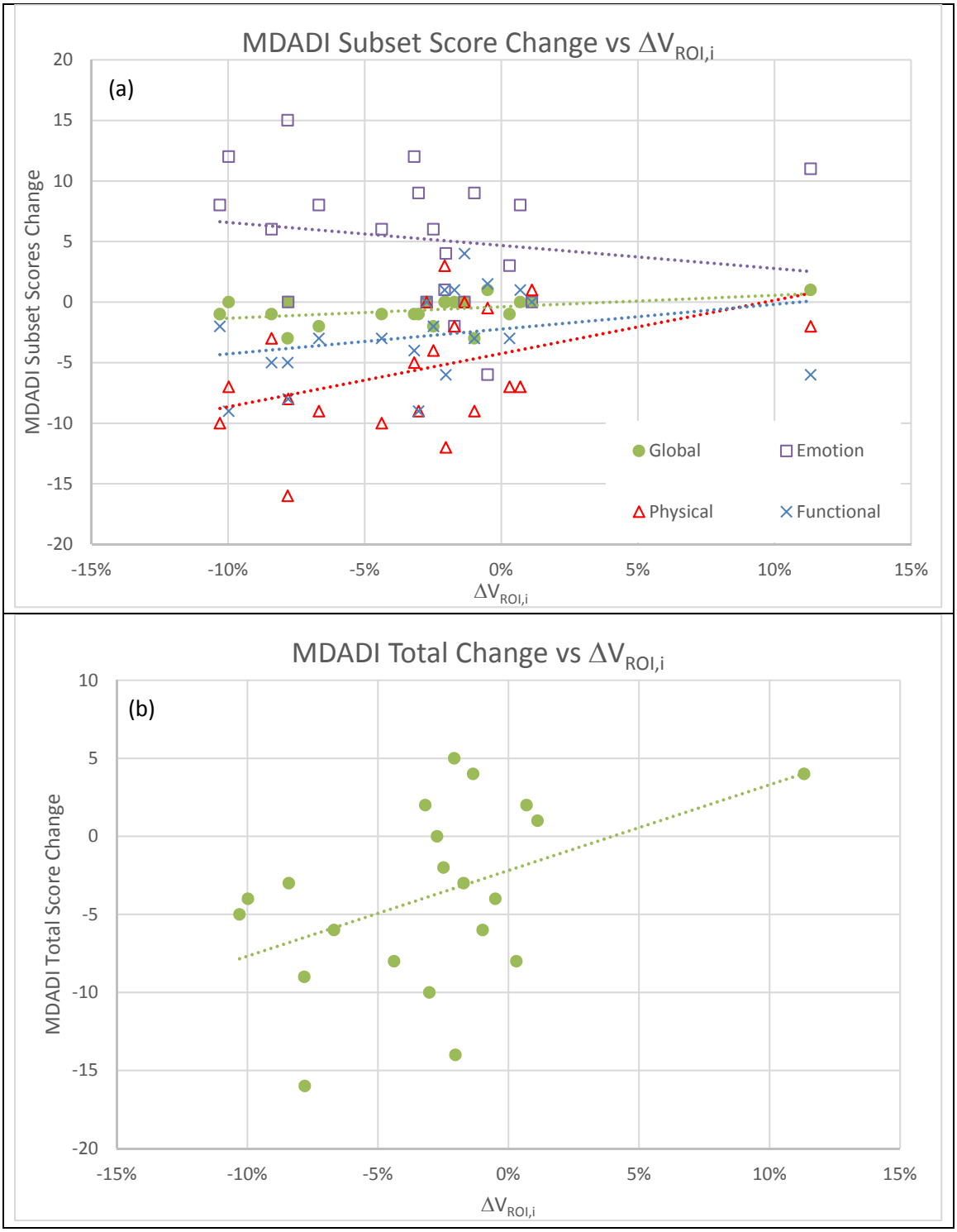

Figure 19: The relationship of $\Delta V_{ROI,i}$ with the MDADI change (a) subsets and (b) total.

Table 9: Rank Pearson correlation of MDADI scores and $\Delta V_{ROI,i}$

$\Delta V_{ROI,i}$	spearman rank correlation				
	Global	Emotion	Physical	Functional	Total
ρ	0.44	-0.34	0.47	0.44	0.40
95% CI	0.90	0.12	0.93	0.90	0.86
	-0.02	-0.80	0.01	-0.02	-0.06
p-value	0.045	0.129	0.032	0.045	0.073

4.5.6 Transit Fluence Change $< \Delta\phi_{e,i}>$

The scatter plots of $<\Delta\phi_{e,i}>$ with MDADI subsets and total changes were plotted in Figure 20a and b respectively. The ranked $< \Delta\phi_{e,i}>$ was calculated and tableted in Table 17 in Appendix IV. Table 17 shows the rank correlation between $<\Delta\phi_{e,i}>$ and the MDADI changes. Global, emotion, physical and functional subsets correlation with $<\Delta\phi_{e,i}>$ were found to be -0.35, 0.23, -0.46 and -0.46 respectively. The total MDADI change correlation with $<\Delta\phi_{e,i}>$ was found to be -0.45. The p-values for two subsets, physical and functional, and total change of MDADI were found to be between 0.036 and 0.038 which are less 0.05 (Table 17). This implies $<\Delta\phi_{e,i}>$ has statistically significant association with these parameters. The statistical power of the correlation with the physical, functional, and total were found to be 0.5, 0.6 and 0.5 respectively.

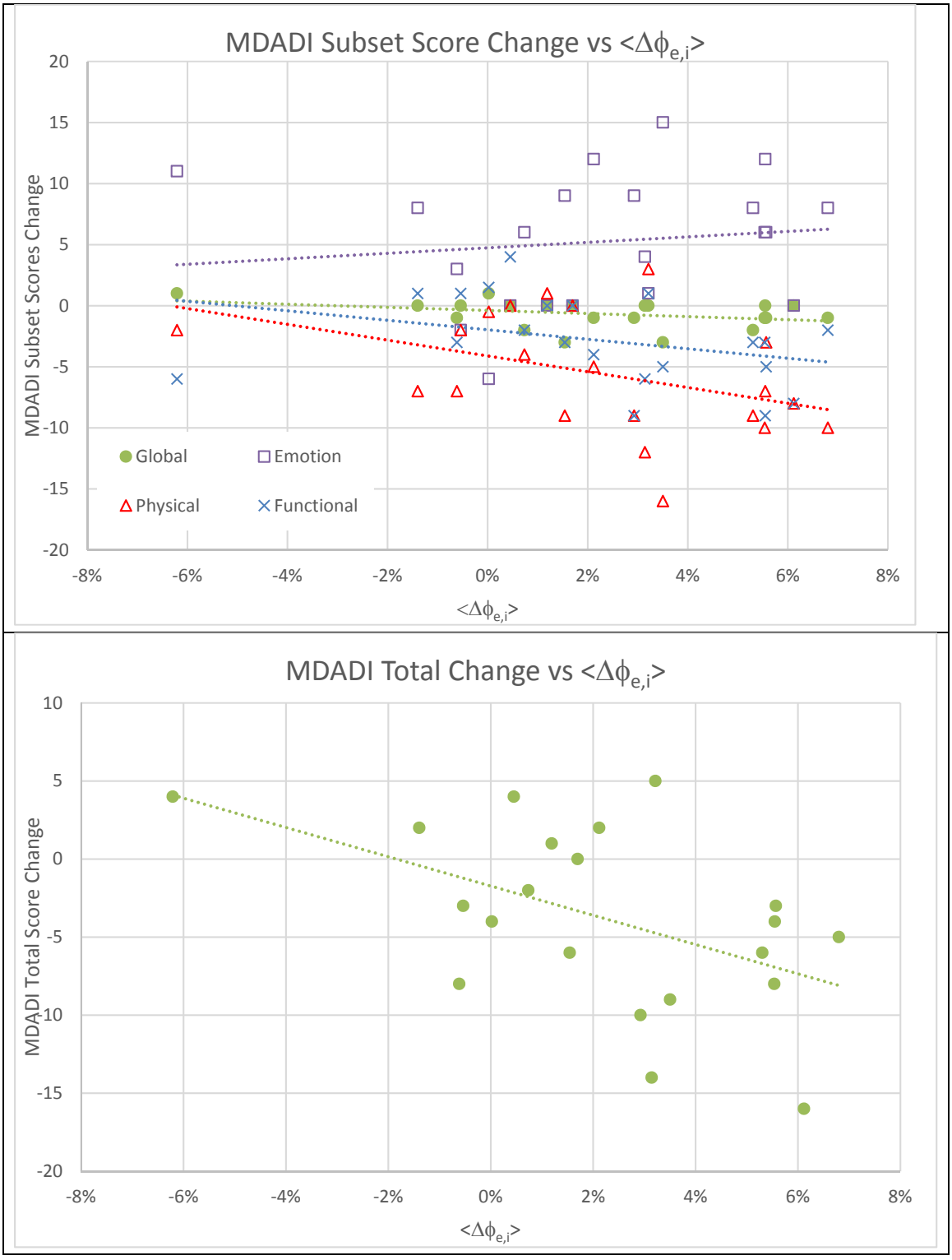

Figure 20: The relationship of <$\Delta\phi_{e,i}$> with the MDADI (a) subsets and (b) total scores change

Table 10: Rank Pearson correlation of MDADI scores and <$\Delta\phi_{e,i}$>

$<\Delta\phi_{e,i}>$	spearman rank correlation				
	Global	Emotion	Physical	Functional	Total
ρ	-0.35	0.23	-0.46	-0.46	-0.45
95% CI	0.11	0.69	0.00	0.01	0.01
	-0.81	-0.24	-0.92	-0.92	-0.92
p-value	0.122	0.324	0.036	0.038	0.038

4.5.7 Salivary Gland Specific Transit Fluence Change $< \Delta\phi_{e,i} > |_{sg}$

Figure 21a and b show the scatter plots between $<\Delta\phi_{e,i}>|_{sg}$ and MDADI subsets and total changes respectively. Table 18 in Appendix IV shows the ranked $<\Delta\phi_{e,i}>|_{sg}$. The rank correlation between $<\Delta\phi_{e,i}>|_{sg}$ and the MDADI changes were calculated and shown in Table 11. The rank correlation between $<\Delta\phi_{e,i}>|_{sg}$ and four subsets, global, emotion, physical and functional, changes were found to be -0.36, 0.17, -0.46 and -0.47. The correlation between $<\Delta\phi_{e,i}>|_{sg}$ and MDADI total change was found to be -0.52. Similar to $<\Delta\phi_{e}>$, the correlation between $<\Delta\phi_{e,i}>|_{sg}$ and two subsets, physical and functional, and total changes were found to have p-values less than 0.05. This implies $<\Delta\phi_{e,i}>|_{sg}$ has statistical significance correlation with these parameters. The statistical power of the correlation with physical, functional and total changes were found to be 0.6, 0.6 and 0.7 respectively.

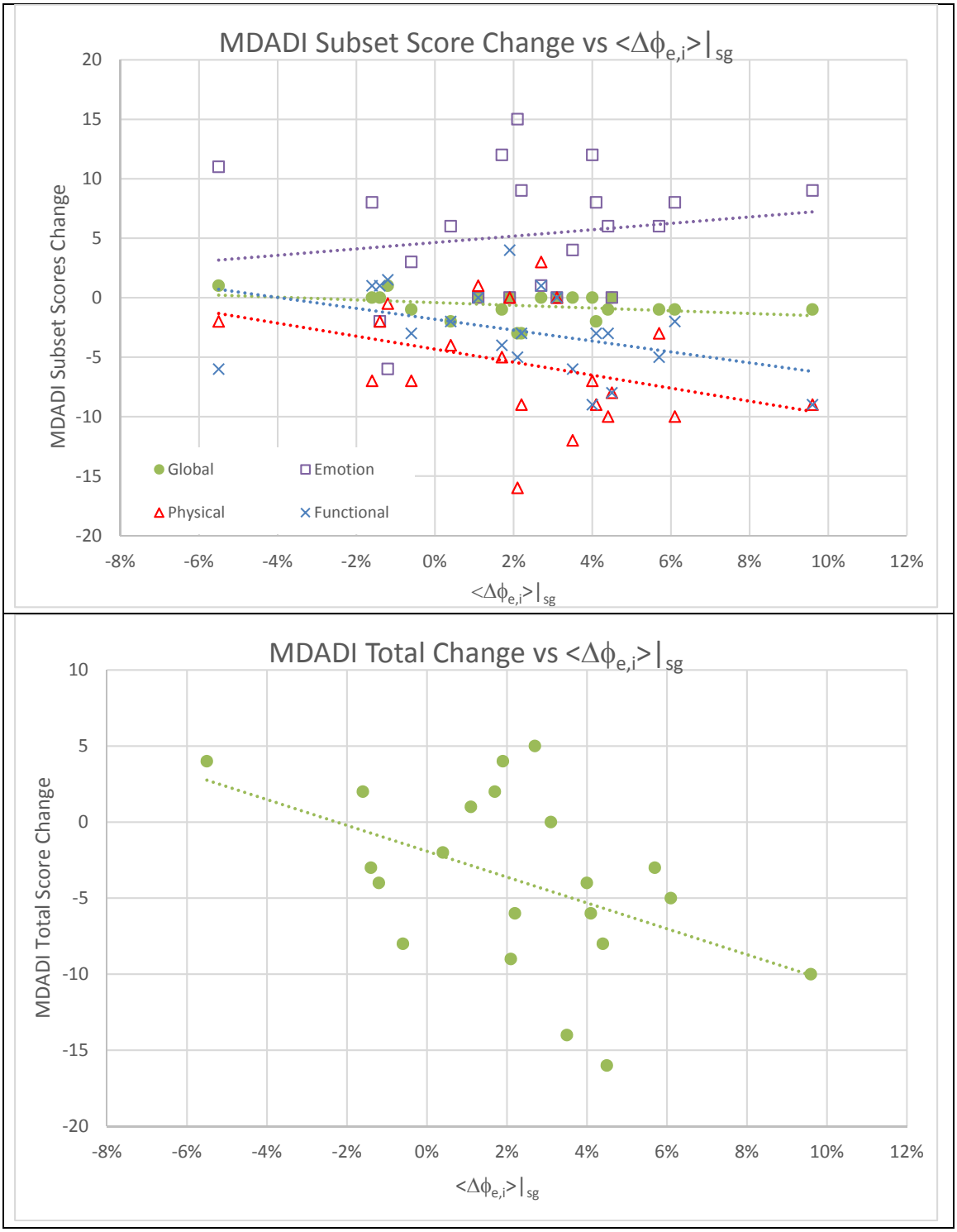

Figure 21: The relationship of $\langle \Delta\phi_{e,i} \rangle|_{sg}$ with the MDADI (a) subsets and (b) total change

Table 11: Rank Pearson correlation of MDADI scores and $<\Delta\phi_{e,i}>|_{sg}$

$<\Delta\phi_{e,i}>\|_{pg}$	spearman rank correlation				
	Global	Emotion	Physical	Functional	Total
ρ	-0.36	0.17	-0.46	-0.47	-0.52
95% CI	0.11	0.63	0.00	-0.01	-0.06
	-0.82	-0.29	-0.92	-0.94	-0.98
p-value	0.113	0.465	0.036	0.030	0.015

Chapter 5

Discussion

The phantom study demonstrated that the DSM is sensitive to change in volume in the neck region. The relationship was found to be negatively correlated. Similar trend was observed in the Phase 1 clinical study.

Over the course of treatment, the change in the transit fluence signal is found to be significantly negatively correlated with the volumetric changes measured by CBCT. The negativity of the correlation can be attributed to the increased transmission of photon fluence with the reduction of radiological pathlength from the decreased volume. The $< \Delta\phi_e >$ correlate reasonably well with the ΔV_{ROI} both in cases where large changes in the volume of the neck ROI and where small changes in the ROI were observed. In the case of patient 1 (Figure 8), the original planning CT was taken a week prior to the beginning of the treatment (arrow "1"). A second CT was taken a week after the start of the treatment (arrow "2") and was used for ART. Both CBCT and WD signal are indicating significant volumetric changes after the 2nd CT was taken. In effect, the CT scan for plan adaption was taken too early. In the cases with volume decrease less than 5%, amount to about 63% of all cases, both CBCT and WD show only minor volumetric change, indicating ART likely to be unnecessary for these patients. Similar to the findings by van Dijk[16] and Marzi[25], the wide timing range of replanning trigger points observed indicates that a pre-determined replanning time may not be an optimal strategy. Coupled with the logistic regression model, this limited data set indicates that WD can provide useful decision support

information to physicians to determine if ART is necessary and a more precise timing of ART without incurring more resources.

From the linear regression analysis, the ROI volume change accounts for about 71% of the change in transit fluence. The change of fluence is associated with the average change in radiological pathlength. The correlation between the change of fluence and volume depends on the shape of underlying anatomy with the ROI. The day-to-day variability in patient setup and machine performance will contribute some noise to the transit fluence signal. Both β_0 and β_1 of the logistic regression model are shown to be statistically significant. The high OR shows a strong association between the WD signal change and replanning decision. The AUC of WD also demonstrates that the signal has comparable accuracy and reliability to mammography[84]. As volumetric change is a good predictor for grade 2 xerostomia[20], change in transit fluence has a potential to predict the volumetric changes in during RT and acts a DSM for ART.

Although the ROI of salivary gland specific DSM is often not at the proximity as $<\Delta\phi_{e,i}>$, $<\Delta\phi_{e,i}>|_{sg}$ shows a significant (p-value < 0.001) positive correlation of 0.776 with $<\Delta\phi_{e,i}>$. The correlation between ΔV_{ROI} and $<\Delta\phi_{e,i}>|_{sg}$ is similar to $<\Delta\phi_{e,i}>$. However, unlike the $<\Delta\phi_{e,i}>$, the linear regression shows that $<\Delta\phi_{e,i}>|_{sg}$ accounts for only 38.5% of the changes in ΔV_{ROI}. This can partly be attributed to the relatively smaller area used in the $<\Delta\phi_{e,i}>|_{sg}$ than $<\Delta\phi_{e,i}>$ resulting less sensitivity in fluence change.

Surveying all the parameters, all of them have no significant association with the emotion subset of MDADI. Similar to other studies[14,19], age and gender was found to have

no significant correlation with the change of xerostomia risk. In addition, weight change during treatment was found to have no significant association. On the dosimetric side, planning salivary mean dose only showed weak association. As the planning dose of these patients were already within accepted planning guideline[8] to minimize xerostomia, mean dose to salivary glands was found to be a week predictor of xerostomia risk in line with Galbry's study[58]. More sophisticated dosimetric metric, such as dose gradient or parotid dose change, may be more useful. Investigation into this fall outside the current study.

Although the results do not show as strong correlation as in study by You[20]'s study, $\Delta V_{ROI,i}$ was found to have clinical important trend with the risk of xerostomia and was also found to have statistically significant association with functional and physical change of xerostomia. Reduction in volume in the neck region was found to be associated with the increase risk of xerostomia.

Significant correlation was found between both transit fluence based DSM, $<\Delta\phi_{e,i}>$ and $<\Delta\phi_{e,i}>|_{sg}$, and the MDADI total score change. Looking at the subset decomposition, both DSM's were also found to be associated with the physical and functional subsets of MDADI. This implies that using either DSM as an early ART replanning signal can potentially improve outcome in HNC treatment. Given the relatively less computational demanding implementation of $<\Delta\phi_{e,i}>$, it may hold an advantage over the more computationally intensive salivary specific version in the case of clinical and automation implementation.

The current study is based on relatively small sample of twenty-four patients to demonstrate the feasibility of the metric. This is the main contributing factor to the relatively low statistical power of the correlation in the xerostomia risk part of the study (ranging from 0.5 to 0.7). A larger data set will be beneficial to further verify the relationship between clinical outcome and the DSM. To obtain a statistical power of 0.8, it is estimated that an additional 20 patients would be needed. Automation of this analysis process can expedite the current labor-intensive ART workflow and broaden its clinical implementation.

Chapter 6

Conclusions and Future Works

The statistically significant negative correlation, observed in the phantom and the clinical study, between $< \Delta\phi_{e,i} >$ and ΔV_{ROI} is attributed to the increase in the photon fluence transport resulting from the ROI volume reduction. The statistically significant association between MDADI score changes and the transit fluence based DSM's verify the clinical impact of using these DSM's as early replanning triggers. Change in transit fluence over the course of treatment can likely be used as a DSM for clinicians to expedite the patient selection for replanning in ART without the need for serial CBCT. Clinical verification of using fluence based DSM replanning trigger on xerostomia risk will be very beneficial.

Current study was carried out using a relatively small sample of twenty-four patients. Larger sample size will be helpful in determining the reproducibility of the transit fluence DSM's and their association with quality of life in patients.

The automation implementation of the DSM's in the clinical workflow was not the focus of the current study. However, such an automatically acquired metric would greatly assist physicians in the difficult task of deciding if, and when a patient's RT plan needed to be adapted to changing anatomy of the tissues being treated and support a broader based ART implementation.

Chapter 7

References

1. Cooper JS, Fu K, Marks J, Silverman S. LATE EFFECTS OF RADIATION-THERAPY IN THE HEAD AND NECK REGION. *Int J Radiat Oncol Biol Phys.* 1995;31(5):1141-1164.

2. Ling CC, Burman C, Chui CS, et al. Conformal radiation treatment of prostate cancer using inversely-planned intensity-modulated photon beams produced with dynamic multileaf collimation. *Int J Radiat Oncol Biol Phys.* 1996;35(4):721-730.

3. Hunt MA, Zelefsky MJ, Wolden S, et al. Treatment planning and delivery of intensity-modulated radiation therapy for primary nasopharynx cancer. *Int J Radiat Oncol Biol Phys.* 2001;49(3):623-632.

4. Lee N, Xia P, Quivey JM, et al. Intensity-modulated radiotherapy in the treatment of nasopharyngeal carcinoma: An update of the UCSF experience. *Int J Radiat Oncol Biol Phys.* 2002;53(1):12-22.

5. Nutting CM, Morden JP, Harrington KJ, et al. Parotid-sparing intensity modulated versus conventional radiotherapy in head and neck cancer (PARSPORT): a phase 3 multicentre randomised controlled trial. *Lancet Oncol.* 2011;12(2):127-136.

6. Castadot P, Lee JA, Geets X, Gregoire V. Adaptive Radiotherapy of Head and Neck Cancer. *Semin Radiat Oncol.* 2010;20(2):84-93.

7. Dijkema T, Raaijmakers CPJ, Ten Haken RK, et al. PAROTID GLAND FUNCTION AFTER RADIOTHERAPY: THE COMBINED MICHIGAN AND UTRECHT EXPERIENCE. *Int J Radiat Oncol Biol Phys.* 2010;78(2):449-453.

8. Deasy JO, Moiseenko V, Marks L, Chao KSC, Nam J, Eisbruch A. RADIOTHERAPY DOSE-VOLUME EFFECTS ON SALIVARY GLAND FUNCTION. *Int J Radiat Oncol Biol Phys.* 2010;76(3):S58-S63.

9. Brouwer CL, Steenbakkers R, Langendijk JA, Sijtsema NM. Identifying patients who may benefit from adaptive radiotherapy: Does the literature on anatomic and dosimetric changes in head and neck organs at risk during radiotherapy provide information to help? *Radiother Oncol.* 2015;115(3):285-294.

10. Brown E, Owen R, Harden F, et al. Predicting the need for adaptive radiotherapy in head and neck cancer. *Radiotherapy and oncology : journal of the European Society for Therapeutic Radiology and Oncology.* 2015;116(1):57-63.

11. Castelli J, Simon A, Louvel G, et al. Impact of head and neck cancer adaptive radiotherapy to spare the parotid glands and decrease the risk of xerostomia. *Radiation oncology (London, England).* 2015;10:6.

12. Guidi G, Maffei N, Meduri B, et al. A machine learning tool for re-planning and adaptive RT: A multicenter cohort investigation. *Phys Medica.* 2016;32(12):1659-1666.

13. Chao KSC, Deasy JO, Markman J, et al. A prospective study of salivary function sparing in patients with head-and-neck cancers receiving intensity-modulated or three-dimensional radiation therapy: Initial results. *Int J Radiat Oncol Biol Phys.* 2001;49(4):907-916.

14. Hawkins PG, Lee JY, Mao YP, et al. Sparing all salivary glands with IMRT for head and neck cancer: Longitudinal study of patient-reported xerostomia and head-and-neck quality of life. *Radiother Oncol.* 2018;126(1):68-74.

15. Lee SW, Kang KW, Wu HG. Prospective investigation and literature review of tolerance dose on salivary glands using quantitative salivary gland scintigraphy in the intensity-modulated radiotherapy era. *Head Neck-J Sci Spec Head Neck.* 2016;38:E1746-E1755.

16. van Dijk LV, Brouwer CL, van der Laan HP, et al. Geometric Image Biomarker Changes of the Parotid Gland Are Associated With Late Xerostomia. *Int J Radiat Oncol Biol Phys.* 2017;99(5):1101-1110.

17. van Dijk LV, Brouwer CL, van der Schaaf A, et al. CT image biomarkers to improve patient-specific prediction of radiation-induced xerostomia and sticky saliva. *Radiother Oncol.* 2017;122(2):185-191.

18. Belli ML, Scalco E, Sanguineti G, et al. Early changes of parotid density and volume predict modifications at the end of therapy and intensity of acute xerostomia. *Strahlenther Onkol.* 2014;190(11):1001-1007.

19. Sanguineti G, Ricchetti F, Wu B, McNutt T, Fiorino C. Parotid gland shrinkage during IMRT predicts the time to Xerostomia resolution. *Radiat Oncol.* 2015;10:6.

20. You SH, Kim SY, Lee CG, et al. Is There a Clinical Benefit to Adaptive Planning During Tomotherapy in Patients with Head and Neck Cancer at Risk for Xerostomia? *Am J Clin Oncol-Cancer Clin Trials.* 2012;35(3):261-266.

21. Schwartz DL, Garden AS, Thomas J, et al. Adaptive Radiotherapy for Head-and-Neck Cancer: Initial Clinical Outcomes From a Prospective Trial. *Int J Radiat Oncol Biol Phys.* 2012;83(3):986-993.

22. Vissink A, van Luijk P, Langendijk JA, Coppes RP. Current ideas to reduce or salvage radiation damage to salivary glands. *Oral Diseases.* 2015;21(1):E1-E10.

23. Wu Q, Chi Y, Chen PY, Krauss DJ, Yan D, Martinez A. Adaptive Replanning Strategies Accounting for Shrinkage in Head and Neck IMRT. *International Journal of Radiation Oncology*Biology*Physics.* 2009;75(3):924-932.

24. Zhang P, Simon A, Rigaud B, et al. Optimal adaptive IMRT strategy to spare the parotid glands in oropharyngeal cancer. *Radiotherapy and oncology : journal of the European Society for Therapeutic Radiology and Oncology.* 2016;120(1):41-47.

25. Marzi S, Pinnaro P, D'Alessio D, et al. Anatomical and Dose Changes of Gross Tumour Volume and Parotid Glands for Head and Neck Cancer Patients during Intensity-modulated Radiotherapy: Effect on the Probability of Xerostomia Incidence. *Clin Oncol.* 2012;24(3):E54-E62.

26. Fuangrod T, Greer PB, Woodruff HC, et al. Investigation of a real-time EPID-based patient dose monitoring safety system using site-specific control limits. *Radiat Oncol.* 2016;11:10.

27. Rozendaal RA, Mijnheer B, Hamming-Vrieze O, Mans A, van Herk M. Impact of daily anatomical changes on EPID-based in vivo dosimetry of VMAT treatments of head-and-neck cancer. *Radiother Oncol.* 2015;116(1):70-74.

28. Rozendaal RA, Mijnheer BJ, van Herk M, Mans A. In vivo portal dosimetry for head-and-neck VMAT and lung IMRT: Linking gamma-analysis with differences in dose-volume histograms of the PTV. *Radiother Oncol.* 2014;112(3):396-401.

29. Woodruff HC, Fuangrod T, Van Uytven E, et al. First Experience With Real-Time EPID-Based Delivery Verification During IMRT and VMAT Sessions. *Int J Radiat Oncol Biol Phys.* 2015;93(3):516-522.

30. Guggenheimer J, Moore PA. Xerostomia - Etiology, recognition and treatment. *J Am Dent Assoc.* 2003;134(1):61-69.

31. Hanchanale S, Adkinson L, Daniel S, Fleming M, Oxberry SG. Systematic literature review: xerostomia in advanced cancer patients. *Supportive Care in Cancer.* 2015;23(3):881-888.

32. Mortazavi H, Baharvand M, Movahhedian A, Mohammadi M, Khodadoustan A. Xerostomia due to systemic disease: a review of 20 conditions and mechanisms. *Annals of medical and health sciences research.* 2014;4(4):503-510.

33. Cheng SC, Wu VW, Kwong DL, Ying MT. Assessment of post-radiotherapy salivary glands. *The British journal of radiology.* 2011;84(1001):393-402.

34. Humphrey SP, Williamson RT. A review of saliva: Normal composition, flow, and function. *J Prosthet Dent.* 2001;85(2):162-169.

35. Eisbruch A, Rhodus N, Rosenthal D, et al. How should we measure and report radiotherapy-induced xerostomia? *Semin Radiat Oncol.* 2003;13(3):226-234.

36. Izumi M, Eguchi K, Nakamura H, Nagataki S, Nakamura T. Premature fat deposition in the salivary glands associated with Sjogren syndrome: MR and CT evidence. *Am J Neuroradiol.* 1997;18(5):951-958.

37. Savage NW, Kruger BJ, Adkins KF. THE EFFECTS OF FRACTIONATED MEGAVOLTAGE X-IRRADIATION ON THE RAT SUBMANDIBULAR-GLAND - AN ASSESSMENT BY ELECTRON-MICROSCOPY. *Aust Dent J.* 1985;30(3):188-193.

38. Stephens LC, Ang KK, Schultheiss TE, King GK, Brock WA, Peters LJ. TARGET-CELL AND MODE OF RADIATION-INJURY IN RHESUS SALIVARY-GLANDS. *Radiother Oncol.* 1986;7(2):165-174.

39. Hall EJ. *Radiobiology for the radiologist.* 3rd ed. ed. Philadelphia: Lippincott; 1988.

40. Teshima K, Murakami R, Tomitaka E, et al. Radiation-induced Parotid Gland Changes in Oral Cancer Patients: Correlation Between Parotid Volume and Saliva Production. *Jpn J Clin Oncol.* 2010;40(1):42-46.

41. Beetz I, Steenbakkers RJ, Chouvalova O, et al. The QUANTEC criteria for parotid gland dose and their efficacy to prevent moderate to severe patient-rated xerostomia. *Acta oncologica (Stockholm, Sweden).* 2014;53(5):597-604.

42. Afzelius P, Nielsen MY, Ewertsen C, Bloch KP. Imaging of the major salivary glands. *Clin Physiol Funct Imaging.* 2016;36(1):1-10.

43. Teshima K, Murakami R, Yoshida R, et al. Histopathological Changes in Parotid and Submandibular Glands of Patients Treated with Preoperative Chemoradiation Therapy for Oral Cancer. *J Radiat Res.* 2012;53(3):492-496.

44. Kohler PF, Winter ME. A quantitative test for xerostomia. The Saxon test, an oral equivalent of the Schirmer test. *Arthritis and rheumatism.* 1985;28(10):1128-1132.

45. Navazesh M. METHODS FOR COLLECTING SALIVA. *Ann NY Acad Sci.* 1993;694:72-77.

46. Wolbarst AB. *Medical imaging essentials for physicians.* First edition. ed. Hoboken, N.J.: Wiley-Blackwell; 2013.

47. Nomayr A, Lell M, Sweeney R, Bautz W, Lukas P. MRI appearance of radiation-induced changes of normal cervical tissues. *Eur Radiol.* 2001;11(9):1807-1817.

48. Cornec D, Jousse-Joulin S, Pers JO, et al. Contribution of salivary gland ultrasonography to the diagnosis of Sjogren's syndrome: Toward new diagnostic criteria? *Arthritis and rheumatism.* 2013;65(1):216-225.

49. Astreinmou E, Roesink JM, Raaijmakers CPJ, et al. 3D MR sialography as a tool to investigate radiation-induced xerostomia: Feasibility study. *Int J Radiat Oncol Biol Phys.* 2007;68(5):1310-1319.

50. Bushberg JT. *The essential physics of medical imaging.* Philadelphia : Wolters Kluwer Health/Lippincott Williams & Wilkins, [2012],Third edition.; 2012.

51. Cannon B, Schwartz DL, Dong L. Metabolic Imaging Biomarkers of Postradiotherapy Xerostomia. *Int J Radiat Oncol Biol Phys.* 2012;83(5):1609-1616.

52. van Dijk LV, Noordzij W, Brouwer CL, et al. F-18-FDG PET image biomarkers improve prediction of late radiation-induced xerostomia. *Radiother Oncol.* 2018;126(1):89-95.

53. Kutcher GJ, Burman C. CALCULATION OF COMPLICATION PROBABILITY FACTORS FOR NON-UNIFORM NORMAL TISSUE IRRADIATION - THE EFFECTIVE VOLUME METHOD. *Int J Radiat Oncol Biol Phys.* 1989;16(6):1623-1630.

54. Lyman JT. COMPLICATION PROBABILITY AS ASSESSED FROM DOSE VOLUME HISTOGRAMS. *Radiat Res.* 1985;104(2):S13-S19.

55. Beetz I, Schilstra C, van der Schaaf A, et al. NTCP models for patient-rated xerostomia and sticky saliva after treatment with intensity modulated radiotherapy for head and neck cancer: The role of dosimetric and clinical factors. *Radiother Oncol.* 2012;105(1):101-106.

56. Brouwer CL, Steenbakkers R, van der Schaaf A, et al. Selection of head and neck cancer patients for adaptive radiotherapy to decrease xerostomia. *Radiother Oncol.* 2016;120(1):36-40.

57. Cox JD, Stetz J, Pajak TF. Toxicity criteria of the Radiation Therapy Oncology Group (RTOG) and the European Organization for Research and Treatment of Cancer (EORTC). *International journal of radiation oncology, biology, physics.* 1995;31(5):1341-1346.

58. Gabrys HS, Buettner F, Sterzing F, Hauswald H, Bangert M. Parotid gland mean dose as a xerostomia predictor in low-dose domains. *Acta Oncol.* 2017;56(9):1197-1203.

59. Nishimura Y, Nakamatsu K, Shibata T, et al. Importance of the initial volume of parotid glands in xerostomia for patients with head and neck cancers treated with IMRT. *Jpn J Clin Oncol.* 2005;35(7):375-379.

60. Hanley O, Leech M. Reduction of xerostomia in head and neck cancer patients. A critical review of the literature. *Radiography.* 2016;22:S57-S63.

61. Chen AY, Frankowski R, Bishop-Leone J, et al. The Development and Validation of a Dysphagia-Specific Quality-of-Life Questionnaire for Patients With Head and Neck Cancer: The M. D. Anderson Dysphagia Inventory. *JAMA Otolaryngology–Head & Neck Surgery.* 2001;127(7):870-876.

62. Dwivedi RC, Chisholm EJ, Khan AS, et al. An exploratory study of the influence of clinico-demographic variables on swallowing and swallowing-related quality of life in a cohort of oral and oropharyngeal cancer patients treated with primary surgery. *Eur Arch Oto-Rhino-Laryn.* 2012;269(4):1233-1239.

63. Orlandi E, Miceli R, Infante G, et al. Predictors of Patient-Reported Dysphagia Following IMRT Plus Chemotherapy in Oropharyngeal Cancer. *Dysphagia.* 2019;34(1):52-62.

64. Sinclair CF, McColloch NL, Carroll WR, Rosenthal EL, Desmond RA, Magnuson JS. Patient-Perceived and Objective Functional Outcomes Following Transoral Robotic Surgery for Early Oropharyngeal Carcinoma. *Arch Otolaryngol Head Neck Surg.* 2011;137(11):1112-1116.

65. Pavy JJ, Denekamp J, Letschert J, et al. LATE EFFECTS TOXICITY SCORING - THE SOMA SCALE. *Radiother Oncol.* 1995;35(1):11-15.

66. Denis F, Garaud P, Bardet E, et al. Late toxicity results of the Gortec 94-01 randomized trial comparing radiotherapy with concomitant radiochemotherapy for advanced-stage oropharynx carcinoma: Comparison of LENT/SOMA, RTOG/EORTC, and NCI-CTC scoring systems. *Int J Radiat Oncol Biol Phys.* 2003;55(1):93-98.

67. Ho KF, Farnell DJJ, Routledge JA, et al. Comparison of patient-reported late treatment toxicity (LENT-SOMA) with quality of life (EORTC QLQ-C30 and QLQ-H&N35) assessment after head and neck radiotherapy. *Radiother Oncol.* 2010;97(2):270-275.

68. Hoeller U, Tribius S, Kuhlmey A, Grader K, Fehlauer F, Alberti W. Increasing the rate of late toxicity by changing the score? A comparison of RTOG/EORTC and LENT/SOMA scores. *Int J Radiat Oncol Biol Phys.* 2003;55(4):1013-1018.

69. Meirovitz A, Murdoch-Kinch CA, Schipper M, Pan C, Eisbruch A. Grading xerostomia by physicians or by patients after intensity-modulated radiotherapy of head-and-neck cancer. *International journal of radiation oncology, biology, physics.* 2006;66(2):445-453.

70. Trotti A, Colevas AD, Setser A, et al. CTCAE v3.0: development of a comprehensive grading system for the adverse effects of cancer treatment. *Semin Radiat Oncol.* 2003;13(3):176-181.

71. Yu CX. INTENSITY-MODULATED ARC THERAPY WITH DYNAMIC MULTILEAF COLLIMATION - AN ALTERNATIVE TO TOMOTHERAPY. *Phys Med Biol.* 1995;40(9):1435-1449.

72. Bzdusek K, Friberger H, Eriksson K, Hardemark B, Robinson D, Kaus M. Development and evaluation of an efficient approach to volumetric arc therapy planning. *Med Phys.* 2009;36(6):2328-2339.

73. Barker JL, Jr., Garden AS, Ang KK, et al. Quantification of volumetric and geometric changes occurring during fractionated radiotherapy for head-and-neck cancer using an

integrated CT/linear accelerator system. *International Journal of Radiation Oncology • Biology • Physics.*59(4):960-970.

74. Bhide SA, Davies M, Burke K, et al. Weekly Volume and Dosimetric Changes During Chemoradiotherapy With Intensity-Modulated Radiation Therapy for Head and Neck Cancer: A Prospective Observational Study. *International Journal of Radiation Oncology*Biology*Physics.* 2010;76(5):1360-1368.

75. Lee C, Langen KM, Lu W, et al. Evaluation of geometric changes of parotid glands during head and neck cancer radiotherapy using daily MVCT and automatic deformable registration. *Radiother Oncol.* 2008;89(1):81-88.

76. Nishi T, Nishimura Y, Shibata T, Tamura M, Nishigaito N, Okumura M. Volume and dosimetric changes and initial clinical experience of a two-step adaptive intensity modulated radiation therapy (IMRT) scheme for head and neck cancer. *Radiother Oncol.* 2013;106(1):85-89.

77. Palma D, Vollans E, James K, et al. VOLUMETRIC MODULATED ARC THERAPY FOR DELIVERY OF PROSTATE RADIOTHERAPY: COMPARISON WITH INTENSITY-MODULATED RADIOTHERAPY AND THREE-DIMENSIONAL CONFORMAL RADIOTHERAPY. *Int J Radiat Oncol Biol Phys.* 2008;72(4):996-1001.

78. Otto K. Volumetric modulated arc therapy: IMRT in a single gantry arc. *Med Phys.* 2008;35(1):310-317.

79. Pota M, Scalco E, Sanguineti G, et al. Early prediction of radiotherapy-induced parotid shrinkage and toxicity based on CT radiomics and fuzzy classification. *Artificial intelligence in medicine.* 2017;81:41-53.

80. Bakai A, Alber M, Nusslin F. A revision of the gamma-evaluation concept for the comparison of dose distributions. *Phys Med Biol.* 2003;48(21):3543-3553.

81. Low DA, Harms WB, Mutic S, Purdy JA. A technique for the quantitative evaluation of dose distributions. *Med Phys.* 1998;25(5):656-661.

82. Vasavada AN, Danaraj J, Siegmund GP. Head and neck anthropometry, vertebral geometry and neck strength in height-matched men and women. *Journal of biomechanics.* 2008;41(1):114-121.

83. Bland M. *An introduction to medical statistics.* 3rd ed. ed. Oxford ;: Oxford University Press; 2000.

84. Swets JA. Measuring the accuracy of diagnostic systems. *Science (New York, NY).* 1988;240(4857):1285-1293.

Appendix I

IRB Letter

Memorial Sloan Kettering Cancer Center
IRB Number: 18-257
Approval date: 18-May-2018

INSTRUCTIONS

- This form should be used for projects that are limited to research using existing data, including waiver of consent and waiver of HIPAA authorization.
- All new research applications must be reviewed and approved by the appropriate primary department prior to submission to the IRB/PB.
- All applications must be typewritten.

PART A. STUDY INFORMATION

Principal Investigator Name:	Michael Lovelock, PhD	
Principal Investigator Department:	Medical Physics	
Principal Investigator Service:	Clinical Physics	
IRB Protocol Number:	18-257	
IRB Protocol Title:	Can a Change in Transit Fluence during Treatment be used to Indicate the Need for Plan Adaptation?	
Investigator(s) Name/Department	Seng Bo Lim, PhD (co-PI)	Medical Physics
Study Contact Name:	Christian Czmielewski	
Study Clinical Research Manager Name:	Nicole Ostrowsky-Fabisch	
Sponsor/Funder:	MSK	
Does this protocol include participants <18 years old?	☐ Yes ☒ No	
Is this a multicenter protocol?	☐ Yes ☒ No	
Anticipated number of individuals whose records will be reviewed?	50	

1.0 STUDY DESCRIPTION

1.1 Background and Rationale

Patients receiving radiotherapy for head and and neck cancer may lose weight during their treatment course. The effect of the weight loss is to change the anatomy in the vicinity of the target. Thus, for the proportion of patients who do lose weight, there is a risk that the radiation dose distribution that is delivered to the patient will differ from that planned. Monitoring patients for weight loss and anatomic change involves the analysis of volumetric scans, either CBCT or MRI, and as such involves significant clinical effort. In this retrospective analysis, the weight loss in the vicinity of the tumor will be correlated with a metric that can be obtained automatically with minimal effort: the transit fluence. The transit fluence is the beam that exits the patient during dose delivery. If anatomic change in the vicinity of the target occurs, the transit fluence will no longer match that expected from the patient's plan. Anatomic change may also result in structures such as salivary glands moving their position with respect to the radiation fields. This may result in them receiving a higher dose than planned, possibly causing the patient to have reduced salivary function.

The primary goal of this work is to investigate the correlation between change in transit fluence and weight loss in the treated region. Such correlation would indicate that transit fluence could be used as an automatic metric generated daily that could be used by the adaptive planning group. The metric would be used to decide when, if at all, a plan adaption is required.

A secondary objective will be to investigate the correlation between the change in transit fluence and a patient's salivary function. This part of the study will involve examining records of the patients self reporting of salivary function.

1.2 Study Objectives

- Quantify the correlation between change in transit fluence and weight loss in the vicinity of the target
- Quantify the correlation between change in transit fluence and salivary function, as reported by patient self assessment forms

1.3 Study Design and Procedures

Analyze treatment records of patients receiving radiotherapy for head and neck cancer. Records from patients treated after January 1, 2016 are eligibile. Records from patient self reports and from follow up visits will be examined. This analysis will involve the extraction of records from about 50 patients.

1.4 Data Collection Procedures

Transit fluence, that is the beam after it has passed through the patient, is collected as part of safety and QA process for dose delivery at specific treatment machines. The transit fluence records will be extracted for patients treated at these two machines.

CBCT scans will be extracted from the Radiation Oncology Record and Verify database: ARIA.

Treatment plans will be extracted from the Eclipse Treatment Planning System.

Records from patient followup visits, and and information from questionnaires given to patients concerning salivary function will be examined.

1.5 Data Analysis

The data collected will be directly entered into spread sheets. Using Microsoft Excel software, the corrections distributions will be determined. Measures such as means and percentiles will be computed.

1.6 Statistical Considerations

The data from 50 patients will enable the significance of the transit fluence and weight loss / salivary function correlations to be assessed.

1.7 References

Quality control quantification (QCQ): a tool to measure the value of quality control checks in radiation oncology. Ford EC, Terezakis S, Souranis A, Harris K, Gay H, Mutic S. Int J Radiat Oncol Biol Phys. 2012

Impact of daily anatomical changes on EPID-based in vivo dosimetry of VMAT treatments of head-and-neck cancer. Rozendaal RA, Mijnheer BJ, Hamming-Vrieze O, Mans A, van Herk M. Radiother Oncol. 2015 .

2.0 SOURCE(S) OF DATA

☒	Hospital/medical records (in and out patient)	☒	Medical health records	☒	Physician/clinic records
☐	Lab, pathology and/or radiology results	☐	Data previously collected for research purposes	☒	Interviews/questionnaires (previously collected only)
☐	Billing records	☒	Other ARIA and Eclipse treatment planning system		

3.0 DATES OF RECORDS

a. Please indicate the range of dates of the records that will be reviewed (Dates must be retrospective):

From: 1/1/2016 To: 3/23/2018

4.0 PRIVACY/CONFIDENTIALITY:

a. What data points are you collecting? (For example: date of diagnosis, date of surgery)
Date of first treatment
Date of last treatment
Dates of follow up visits
Date of patient questionares
Treatment planning and patient imaging data
Patient weights

b. Will the data be linked to the source? ☒ Yes ☐ No

c. Data that are coded, where the key to the code is accessible to researchers, are considered protected health information (PHI) and are subject to HIPAA regulations. Will any of the following identifiers be recorded with or linked by code to the data? ☒ Yes ☐ No

If yes, check all that apply:
☒ Names
☒ Medical Record Numbers
☐ Account Numbers
☒ Dates: All elements of dates (except year) for dates related to an individual, including: birth

date, admission date, discharge date, date of death, all ages over 89 and all elements of dates (including year) indicative of such age [see policies for further guidance]

☒ Any other unique identifying numbers, characteristics or codes

If any of the following identifiers are selected, a reason must be included below.

☐ Vehicle identifiers and serial #s (license plate numbers)
☐ Device identifiers and serial numbers
☐ Web Universal Resource Locators (URLs)
☐ Biometric identifiers, including finger and voiceprints
☐ Full face photographic images and any comparable images
☐ All geographic subdivisions smaller than a state, including: street address; city; county; precinct; zip codes and their equivalent geocodes, except the initial three digits of a zip code
☐ Telephone numbers
☐ Fax numbers
☐ Electronic mail addresses
☐ Social security numbers
☐ Health plan beneficiary numbers
☐ Account numbers
☐ Certificate/license number
☐ Internet Protocol (IP) address numbers

Reason for request:

d. Who will have access to the data/health information?

i. MSK (List full name and Department):
Michael Lovelock, PhD - Medical Physics
Seng Boh (Gary) Lim, PhD- Medical Physics

ii. Non-MSK researchers (List full name and affiliation):
N/A

iii. What will be the process for releasing information to non-MSK researchers?
Information will not be releasted to non-MSK researchers.

iv. How will the data be labeled or coded?
Data will be labeled with a study ID number.

v. Will PHI be released? ☐ Yes ☒ No

If yes, a Data Use Agreement (DUA) must be executed prior to data being sent outside of MSK.

e. Describe how the data/health information will be stored. Include the following information: (a) where the identifiable information will be stored, (b) who has access to the storage area, (c) what password protections are enabled, and (d) how access will be monitored.

Data will be stored on password protected MSK network drives. Only the individuals listed on this protocol will have access. Standard MSK IT password protections and access monitoring are enabled.

PART B. REQUEST FOR WAIVER OF INFORMED CONSENT

a. Select or explain why/how this research involves no more than minimal risk to the participants or their privacy. (Minimal risk is defined as the probability and magnitude of harm or discomfort as being no greater than those encountered in daily life or during the performance of routine physical or psychological tests)
- ☐ Research involves individual or groups characteristics or behavior
- ☒ Collection of data through non-invasive procedures
- ☒ Research involving materials (data, documents, records)
- ☐ Collection of data from voice, video, digital or image recordings made for research purposes
- ☐ Other:

b. Select or explain why the waiver or alteration will not adversely affect the rights and welfare of the participants.
- ☒ The research involves minimal risk to the participants
- ☒ The research involves non-invasive procedures
- ☐ Data will be deidentified and destroyed upon completion of the project
- ☒ Other: Data will be de-identified upon completion of the project and stored on a secure MSK network drive.

c. Select or explain why the research could not practicably be carried out without the waiver.
- ☒ The research requires the identification of participants for inclusion (alive and/or deceased)
- ☒ The research requires collection of information of research participants over an extended period of time
- ☐ Other:

d. Select or explain how, whenever appropriate, the participants will be provided with additional pertinent information after participation.
- ☐ Attempts to contact participants will be made if life threatening results are found
- ☒ Other: Patients have already received treatment and will not be contacted as part of this study.

PART C. REQUEST FOR WAIVER OF HIPAA AUTHORIZATION

a. Select or explain why the research could not practicably be conducted without access to and use of the protected health information (PHI):
- ☒ The PHI is needed to answer the retrospective research question
- ☒ The PHI is needed to determine participant eligibility for the research study
- ☒ The PHI is needed to conduct the research analysis
- ☒ Participant records are needed to verify treatment and outcomes
- ☐ Other:

b. Select or explain why the Protected Health Information (PHI) to be used or disclosed is the minimum necessary to accomplish the research objectives:

☒ Only PHI needed to answer research question will be used
☐ Other:

c. Select or explain why the use or disclosure of the PHI involves no more than minimal risk to the privacy of the individuals (check all that apply):
☒ Limited identifiable information
☒ Information (data) maintained in a secure/network location
☒ No plans to distribute identifiable information outside of MSK
☐ Other:

d. The identifiers must be destroyed at the earliest opportunity consistent with conduct of the research, unless there is a health or research justification for retaining the identifiers or such retention is otherwise required by law. Select or describe the plan for destroying the identifiers at or before the conclusion of the study or provide a justification for long term or permanent retention of the identifiers:
☐ No hard copies will be maintained, all data files will be destroyed upon completion of the project
☐ All hard copies will be shredded or discarded in blue confidential recycling bins
☐ All electronic files will be destroyed and/or deleted from the secure network drive
☒ Other: Data will be de-identified and stored on a MSK network drive for future possible research purposes. The databases will be registered with CRA.

e. Describe the measures you will take to ensure the PHI will not be reused or disclosed to any other person or entity, except as required by law, for authorized oversight of the research study, or for other research approved by the IRB:
☐ As noted above, all records will be destroyed and not maintained for future use
☒ Other: Data will be de-identified and stored on a MSK network drive for future possible research purposes. The databases will be registered with CRA.

Appendix II

Matlab Script for Cine Image Conversion

```
%Script of loading every patient data

%written by Gary Seng Boh Lim

%Date = 04/18/2017

%This script convert separate *.mat files into corresponding *.iso files

%for contour overlay



home_path = '\\pisidsmph\PhysicsQA$\Gary\Watchdog Data\442\\';



data_directory_tx = dir(strcat(home_path,'tx*.'));

DataSize = size(data_directory_tx);



for indexDir = 1:DataSize(1)

    if data_directory_tx(indexDir).isdir == 1
```

```
data_directory = strcat(home_path, data_directory_tx(indexDir).name);

%Load all files in the directory

%data_directory = uigetdir(home_path,'Select WD Patient data');

data_directory_mat = dir(strcat(data_directory,'\*.mat'));

%       data_files = dir(data_directory_mat);

data_files = data_directory_mat;

Num_files = length(data_files);



Patient_frames = zeros(384,512);

for index = 1:Num_files

   currentfile = fullfile(data_directory,data_files(index).name);

   load(currentfile);

   currentframe = session.frames;

   currentframe = sum(currentframe,3);

   Patient_frames = Patient_frames + currentframe;
```

```
%Data_result = [Data_result; session.angles; session.results(2,:)];

%data_length = length(session.angles);

%data_length_baseline(index) = data_length;

%Data_baseline(3*index-2,1:data_length) = session.angles;

%Data_baseline(3*index-1, 1:data_length) = session.results(1,:);

%Data_baseline(3*index, 1:data_length) = session.results(2,:);

panelSize= size(Patient_frames);

ISO_pos = [40*2/3/2 30*2/3/2];

pixelSize = 40*2/3/max(panelSize); %at isocenter

ArraySize = panelSize(1)*panelSize(2);

Contour_out = zeros(ArraySize,3);

CAX_dose = Patient_frames(256,192);

currentIndex = 1;

Patient_frames_old = Patient_frames;

%Patient_frames = imrotate(Patient_frames,180);
```

```
%Patient_frames = fliplr(Patient_frames);

for index_r = 1: panelSize(1)

   for index_c = 1:panelSize(2)

      %currentIndex = round(index_r*index_c);

      Contour_out(currentIndex,1)=index_c-1;

      Contour_out(currentIndex,2)=index_r-1;

      Contour_out(currentIndex,3)  =  Patient_frames(index_r,  index_c)/1000;
%scale 1000

      currentIndex = currentIndex +1;

   end

end



outputfile_grid = ['X Grid, Y Grid(cm) =  ' num2str(pixelSize) ' ,   '
num2str(pixelSize) ','];

outputfile_res = [ 'Nx, Ny = 512 ,       384 ,          '];
```

```
outputfile_ISO = [' ISO x, y(cm) and Dose = ' num2str(ISO_pos(1)) ', ' num2str(ISO_pos(2)) ',          ' num2str(CAX_dose)];

outputfile_index = ['i    j          Dose'];



%writing data%

outputfilename = [data_files(index).name(1:27) '-cv.iso'];

outputfile = fullfile(data_directory, outputfilename);

fid = fopen(outputfile,'w+');

fprintf(fid,'%s\r\n',outputfile_grid)

fprintf(fid,'%s\r\n',outputfile_res)

fprintf(fid,'%s\r\n', ' ')

fprintf(fid,'%s\r\n',outputfile_ISO)

fprintf(fid,'%s\r\n', ' ')

fprintf(fid,'%s\r\n',outputfile_index)

fclose(fid);

dlmwrite(outputfile,Contour_out,'-append','delimiter','\t');
```

```
        end

    end

end



%figure('Name', 'Patient Measurement');

%mesh(Patient_frames');



%This script convert WD frames to Contour Overlay

%Panel Size 40x30cm (512x384 pixels)or 26.7x20 at isocenter

%Isocenter position 20cm, 15cm

%need center dose (256, 192)
```

Appendix III

Matlab Script for ROC Analysis

```
%WD ROC Analyais

%WD is the measurement

%RP = replanning trigger based on CBCT volume change

% 1 means replan and 0 means nothing

% Written By Gary S. Lim

% 2018-12-13



close;

clear;

clc;



% WD = [-0.0850000000000000;0.0130000000000000;-0.0340000000000000;-
0.0160000000000000;-0.0210000000000000;-0.0370000000000000;-
```

```
0.0470000000000000;-0.0390000000000000;-0.0420000000000000;-
0.0710000000000000;-
0.0090000000000000;0.0130000000000000;0.0230000000000000;-
0.0210000000000000;-0.0370000000000000;-0.0440000000000000;-
0.0380000000000000;-0.0710000000000000;-0.0310000000000000;-
0.0210000000000000;-0.0320000000000000;-0.0090000000000000;-
0.0260000000000000;-0.0460000000000000;-0.0220000000000000;-
0.0470000000000000;-0.0410000000000000;0.0070000000000000;-
0.0180000000000000;-0.0230000000000000;-0.0440000000000000;-
0.0420000000000000;-0.0310000000000000;-0.0500000000000000;-
0.0480000000000000;-0.0060000000000000;-0.0290000000000000;-
0.0230000000000000;-0.0190000000000000;-
0.0010000000000000;0.0090000000000000;-0.0200000000000000;-
0.0730000000000000;-0.0680000000000000;-
0.0260000000000000;0.0280000000000000];

% WD = -WD;

% %value needs to be > 0

% minWD = min(WD);

% WD = WD - minWD;
```

% RP1 =
[1;1;1;1;1;1;1;1;1;1;1;0;0;1;1;1;1;1;0;1;1;0;1;1;0;1;1;0;1;1;1;1;1;1;1;1;1;1;1;1;0;1;1;1;0;0
]; %threshold = 0.0%

% RP2 =
[1;0;0;0;1;1;1;1;1;1;0;0;0;0;1;1;1;1;0;0;0;0;1;1;0;0;1;0;0;1;1;0;1;0;1;0;1;1;1;0;0;0;1;1;0;0
]; %threshold -2.5%

% RP3 =
[1;0;0;0;0;1;1;0;1;1;0;0;0;0;0;1;1;1;0;0;0;0;0;0;0;0;0;0;0;0;0;0;0;0;0;1;0;1;0;0;0;0;0;1;0;0
]; %threshold = -5.0%

% RP4 =
[1;0;0;0;0;0;1;0;1;1;0;0;0;0;0;0;0;1;0;0;0;0;0;0;0;0;0;0;0;0;0;0;0;0;0;0;0;0;0;0;0;0;0;0;0;0
]; %Threshold = -7.5%

WD = [-0.0900000000000000,0.0270000000000000,-0.0290000000000000,-
0.0080000000000000,-0.0140000000000000,-0.0330000000000000,-
0.0450000000000000,-0.0350000000000000,-0.0380000000000000,-
0.0730000000000000,0.0010000000000000,0.0270000000000000,0.039000000000000
0,-0.0140000000000000,-0.0330000000000000,-0.0410000000000000,-
0.0340000000000000,-0.0730000000000000,-0.0250000000000000,-
0.0130000000000000,-0.0260000000000000,0.0010000000000000,-

0.0200000000000000,-0.0440000000000000,-0.0140000000000000,-
0.0440000000000000,-0.0370000000000000,0.0210000000000000,-
0.0100000000000000,-0.0160000000000000,-0.0410000000000000,-
0.0380000000000000,-0.0260000000000000,-0.0480000000000000,-
0.0460000000000000,0.0050000000000000,-0.0230000000000000,-
0.0160000000000000,-
0.0110000000000000,0.0100000000000000,0.0230000000000000,-
0.0120000000000000,-0.0760000000000000,-0.0700000000000000,-
0.0190000000000000,0.0450000000000000,0.0610000000000000,0.0670000000000000,
0.0250000000000000,0.0670000000000000,0.0420000000000000,0.0800000000000000,
-0.0150000000000000,-0.0100000000000000,-0.0220000000000000,-
0.0270000000000000,-0.0370000000000000,-0.0680000000000000,-
0.0810000000000000,-0.0400000000000000,-
0.0060000000000000,0.0100000000000000,-0.0260000000000000,-
0.0010000000000000,-0.0020000000000000,-0.0080000000000000,-
0.0460000000000000,-0.0170000000000000,-0.0340000000000000,-
0.0410000000000000,-0.0340000000000000,-0.0120000000000000,-
0.0450000000000000,-0.0430000000000000,-0.0710000000000000,-
0.0730000000000000,-0.0120000000000000,0,-
0.0180000000000000,0.0040000000000000,0.0240000000000000,0.029000000000000
0,0.0190000000000000,-0.0030000000000000,-
0.0070000000000000,0.0060000000000000,-
0.0130000000000000,0.0040000000000000,0,0.0060000000000000,-

0.00400000000000000,0.00300000000000000,-
0.00900000000000000,0.0180000000000000,-0.0110000000000000,-
0.0130000000000000,-0.0210000000000000,-0.0400000000000000,-
0.0220000000000000,0.00100000000000000,-
0.00100000000000000,0.0160000000000000,0.0160000000000000,0.012000000000000
0,0,0.00800000000000000,-0.0100000000000000,0.0110000000000000];

WD = -WD;

%value needs to be > 0

minWD = min(WD);

WD = WD - minWD;

RP1 =
[1;1;1;1;1;1;1;1;1;1;1;0;0;1;1;1;1;1;0;1;1;0;1;1;0;1;1;0;1;1;1;1;1;1;1;1;1;1;1;1;0;1;1;1;0;0
;0;0;0;0;0;0;0;1;1;1;1;1;1;1;1;1;1;1;0;1;1;1;1;1;1;1;1;1;1;1;1;1;1;0;1;1;0;0;0;0;1;1;0;1;1;1;1;1
;1;1;1;1;1;1;1;0;0;0;0;0;1;0;1;1]; %threshold = 0.0%

RP2 =
[1;0;0;0;1;1;1;1;1;1;0;0;0;0;1;1;1;1;0;0;0;0;1;1;0;0;1;0;0;1;1;0;1;0;1;0;1;1;1;0;0;0;1;1;0;0
;0;0;0;0;0;0;0;0;1;1;1;1;1;1;0;0;0;1;0;0;0;1;0;0;0;1;1;1;0;1;1;0;0;0;0;0;0;0;0;0;0;0;0;0;0;0;0
;0;0;0;0;1;0;0;0;0;0;0;0;1;0;1;0]; %threshold -2.5%

```
RP3 =
[1;0;0;0;0;1;1;0;1;1;0;0;0;0;0;1;1;1;0;0;0;0;0;0;0;0;0;0;0;0;0;0;0;0;0;1;0;1;0;0;0;0;0;1;0;0
;0;0;0;0;0;0;0;0;0;0;0;1;1;0;0;0;0;0;0;0;0;0;0;0;0;0;0;0;0;0;0;0;0;0;0;0;0;0;0;0;0;0;0;0;0;0
;0;0;0;0;0;0;0;0;0;0;0;0;0;0;0;0;0;0];  %threshold = -5.0%

RP4 =
[1;0;0;0;0;0;1;0;1;1;0;0;0;0;0;0;0;1;0;0;0;0;0;0;0;0;0;0;0;0;0;0;0;0;0;0;0;0;0;0;0;0;0;0;0;0
;0;0;0;0;0;0;0;0;0;0;0;0;0;1;0;0;0;0;0;0;0;0;0;0;0;0;0;0;0;0;0;0;0;0;0;0;0;0;0;0;0;0;0;0;0;0
;0;0;0;0;0;0;0;0;0;0;0;0;0;0;0;0;0;0];  %Threshold = -7.5%



%dummy = zeros(1,35);



RP1 = RP1';

RP2 = RP2';

RP3 = RP3';

RP4 = RP4';

%converting RP into category for analysis
```

```
RP1_out = categorical(RP1);

RP2_out = categorical(RP2);

RP3_out = categorical(RP3);

RP4_out = categorical(RP4);



%Generate a logistic regession for RP1

mdl1 = fitglm(WD, RP1_out, 'Distribution', 'binomial', 'Link', 'logit');

scores1 = mdl1.Fitted.Probability;

[x1, y1, T1, AUC1]=perfcurve(RP1, scores1,'1');



AUC1

figure;

plot(x1,y1, 'r--');

hold;
```

```
%Generate a logistic regession for RP2

mdl2 = fitglm(WD, RP2_out, 'Distribution', 'binomial', 'Link', 'logit');

scores2 = mdl2.Fitted.Probability;

[x2, y2, T2, AUC2]=perfcurve(RP2, scores1,'1');



AUC2

plot(x2,y2, 'g-');



%Generate a logistic regession for RP3

mdl3 = fitglm(WD, RP3_out, 'Distribution', 'binomial', 'Link', 'logit');

scores3 = mdl3.Fitted.Probability;

[x3, y3, T3, AUC3]=perfcurve(RP3, scores1,'1');



AUC3

plot(x3,y3, 'b-');
```

```
%Generate a logistic regession for RP4

mdl4 = fitglm(WD, RP4_out, 'Distribution', 'binomial', 'Link', 'logit');

scores4 = mdl4.Fitted.Probability;

[x4, y4, T4, AUC4]=perfcurve(RP4, scores1,'1');



AUC4

plot(x4,y4, 'k--');



%Plotting AUC = 0.5

x0 = 0:0.1:1;

y0 = x0;

plot(x0, y0, ':');

hold off
```

```
legend(['Th = 0.0% AUC = ' num2str(round(AUC1*100)/100)],['Th = -2.5% AUC = '
num2str(round(AUC2*100)/100)], ['Th = -5.0% AUC = '
num2str(round(AUC3*100)/100)], ['Th = -7.5% AUC = '
num2str(round(AUC4*100)/100)], 'AUC = 0.5');

xlabel('FPR');

ylabel('TPR');

grid;



%Ploting ROC with Threshold = -5.0%

f2 = figure('Name','ROC Plot with Threshold = -5.0%');

plot(x3,y3, 'r');

hold on;

x0 = 0:0.1:1;

y0 = x0;

plot(x0, y0, ':');
```

```
hold off



legend(['\Delta\phi_e, AUC = ' num2str(round(AUC3*100)/100)], 'AUC = 0.5');

xlabel('FPR');

ylabel('TPR');

grid;
```

Appendix IV

Rank Data

Age

Table 12: Ranked data of MDADI change and age

Global	Emotion	Physical	Functional	Total	Age
14.5	8.0	18.5	8.5	13.0	5.5
20.5	1.0	21.0	15.5	18.0	16.0
7.0	2.5	12.0	20.5	11.5	13.0
1.5	21.0	5.0	2.0	11.5	18.0
18.5	11.0	9.0	8.5	8.0	15.0
14.5	11.0	8.0	15.5	9.5	5.5
7.0	17.5	3.5	6.5	7.0	10.5
14.5	5.5	16.0	20.5	19.0	13.0
14.5	2.5	10.0	14.0	4.5	3.0
7.0	8.0	12.0	4.0	4.5	7.5
18.5	8.0	16.0	11.5	14.5	13.0
1.5	4.0	6.5	17.5	2.5	1.0
7.0	17.5	14.0	19.0	21.0	7.5
7.0	17.5	3.5	1.0	2.5	4.0
7.0	15.0	1.0	4.0	1.0	17.0
14.5	11.0	18.5	11.5	16.5	20.0
20.5	5.5	16.0	11.5	14.5	10.5
7.0	17.5	2.0	6.5	6.0	19.0
7.0	13.0	20.0	17.5	20.0	9.0
14.5	14.0	12.0	11.5	16.5	21.0
7.0	20.0	6.5	4.0	9.5	2.0

Gender

Table 13: Ranked data of MDADI change and gender

Global	Emotion	Physical	Functional	Total	Gender
14.5	8.0	18.5	8.5	13.0	8.0
20.5	1.0	21.0	15.5	18.0	8.0
7.0	2.5	12.0	20.5	11.5	8.0
1.5	21.0	5.0	2.0	11.5	8.0
18.5	11.0	9.0	8.5	8.0	8.0
14.5	11.0	8.0	15.5	9.5	8.0
7.0	17.5	3.5	6.5	7.0	18.5
14.5	5.5	16.0	20.5	19.0	18.5
14.5	2.5	10.0	14.0	4.5	8.0
7.0	8.0	12.0	4.0	4.5	18.5
18.5	8.0	16.0	11.5	14.5	8.0
1.5	4.0	6.5	17.5	2.5	8.0
7.0	17.5	14.0	19.0	21.0	8.0
7.0	17.5	3.5	1.0	2.5	8.0
7.0	15.0	1.0	4.0	1.0	18.5
14.5	11.0	18.5	11.5	16.5	8.0
20.5	5.5	16.0	11.5	14.5	8.0
7.0	17.5	2.0	6.5	6.0	8.0
7.0	13.0	20.0	17.5	20.0	18.5
14.5	14.0	12.0	11.5	16.5	8.0
7.0	20.0	6.5	4.0	9.5	18.5

Mean Dose to Salivary Gland

Table 14: Ranked data of MDADI change and mean dose to salivary gland

Global	Emotion	Physical	Functional	Total	$\langle Dose_{SG} \rangle$
14.5	8.0	18.5	8.5	13.0	12.0
20.5	1.0	21.0	15.5	18.0	6.0
7.0	2.5	12.0	20.5	11.5	16.0
1.5	21.0	5.0	2.0	11.5	20.0
18.5	11.0	9.0	8.5	8.0	19.0
14.5	11.0	8.0	15.5	9.5	3.0
7.0	17.5	3.5	6.5	7.0	1.0
14.5	5.5	16.0	20.5	19.0	5.0
14.5	2.5	10.0	14.0	4.5	14.0
7.0	8.0	12.0	4.0	4.5	4.0
18.5	8.0	16.0	11.5	14.5	10.0
1.5	4.0	6.5	17.5	2.5	2.0
7.0	17.5	14.0	19.0	21.0	8.0
7.0	17.5	3.5	1.0	2.5	21.0
7.0	15.0	1.0	4.0	1.0	11.0
14.5	11.0	18.5	11.5	16.5	7.0
20.5	5.5	16.0	11.5	14.5	17.0
7.0	17.5	2.0	6.5	6.0	18.0
7.0	13.0	20.0	17.5	20.0	13.0
14.5	14.0	12.0	11.5	16.5	9.0
7.0	20.0	6.5	4.0	9.5	15.0

Weight Change

Table 15: Ranked data of MDADI and weight change

Global	Emotion	Physical	Functional	Total	∆weight
14.5	8.0	18.5	8.5	13.0	11.0
20.5	1.0	21.0	15.5	18.0	2.0
7.0	2.5	12.0	20.5	11.5	6.0
1.5	21.0	5.0	2.0	11.5	4.0
18.5	11.0	9.0	8.5	8.0	9.0
14.5	11.0	8.0	15.5	9.5	20.0
7.0	17.5	3.5	6.5	7.0	17.0
14.5	5.5	16.0	20.5	19.0	10.0
14.5	2.5	10.0	14.0	4.5	19.0
7.0	8.0	12.0	4.0	4.5	1.0
18.5	8.0	16.0	11.5	14.5	13.0
1.5	4.0	6.5	17.5	2.5	7.0
7.0	17.5	14.0	19.0	21.0	18.0
7.0	17.5	3.5	1.0	2.5	12.0
7.0	15.0	1.0	4.0	1.0	15.0
14.5	11.0	18.5	11.5	16.5	21.0
20.5	5.5	16.0	11.5	14.5	14.0
7.0	17.5	2.0	6.5	6.0	3.0
7.0	13.0	20.0	17.5	20.0	8.0
14.5	14.0	12.0	11.5	16.5	16.0
7.0	20.0	6.5	4.0	9.5	5.0

Volumetric Change in the ROI

Table 16: Ranked data of MDADI change and ΔV_{ROI}

Global	Emotion	Physical	Functional	Total	ΔV_{ROI}
14.5	8.0	18.5	8.5	13.0	21.0
20.5	1.0	21.0	15.5	18.0	18.0
7.0	2.5	12.0	20.5	11.5	20.0
1.5	21.0	5.0	2.0	11.5	5.0
18.5	11.0	9.0	8.5	8.0	11.0
14.5	11.0	8.0	15.5	9.5	19.0
7.0	17.5	3.5	6.5	7.0	12.0
14.5	5.5	16.0	20.5	19.0	13.0
14.5	2.5	10.0	14.0	4.5	14.0
7.0	8.0	12.0	4.0	4.5	3.0
18.5	8.0	16.0	11.5	14.5	16.0
1.5	4.0	6.5	17.5	2.5	1.0
7.0	17.5	14.0	19.0	21.0	17.0
7.0	17.5	3.5	1.0	2.5	7.0
7.0	15.0	1.0	4.0	1.0	10.0
14.5	11.0	18.5	11.5	16.5	15.0
20.5	5.5	16.0	11.5	14.5	6.0
7.0	17.5	2.0	6.5	6.0	2.0
7.0	13.0	20.0	17.5	20.0	9.0
14.5	14.0	12.0	11.5	16.5	4.0
7.0	20.0	6.5	4.0	9.5	8.0

Average Transit Fluence Change

Table 17: Ranked data of MDADI change and $<\Delta\phi_e>$

Global	Emotion	Physical	Functional	Total	$<\Delta\phi_e>$
14.5	8.0	18.5	8.5	13.0	1.0
20.5	1.0	21.0	15.5	18.0	7.0
7.0	2.5	12.0	20.5	11.5	4.0
1.5	21.0	5.0	2.0	11.5	17.0
18.5	11.0	9.0	8.5	8.0	15.0
14.5	11.0	8.0	15.5	9.5	3.0
7.0	17.5	3.5	6.5	7.0	12.0
14.5	5.5	16.0	20.5	19.0	10.0
14.5	2.5	10.0	14.0	4.5	11.0
7.0	8.0	12.0	4.0	4.5	20.0
18.5	8.0	16.0	11.5	14.5	6.0
1.5	4.0	6.5	17.5	2.5	21.0
7.0	17.5	14.0	19.0	21.0	2.0
7.0	17.5	3.5	1.0	2.5	16.0
7.0	15.0	1.0	4.0	1.0	8.0
14.5	11.0	18.5	11.5	16.5	5.0
20.5	5.5	16.0	11.5	14.5	13.0
7.0	17.5	2.0	6.5	6.0	14.0
7.0	13.0	20.0	17.5	20.0	9.0
14.5	14.0	12.0	11.5	16.5	19.0
7.0	20.0	6.5	4.0	9.5	18.0

Salivary Gland Masked Transit Fluence

Table 18: Ranked data of MDADI change and $<\Delta\phi_e>|_{sg}$

Global	Emotion	Physical	Functional	Total	$<\Delta\phi_e>\|_{sg}$
14.5	8.0	18.5	8.5	13.0	2.0
20.5	1.0	21.0	15.5	18.0	12.0
7.0	2.5	12.0	20.5	11.5	7.0
1.5	21.0	5.0	2.0	11.5	18.0
18.5	11.0	9.0	8.5	8.0	16.0
14.5	11.0	8.0	15.5	9.5	3.0
7.0	17.5	3.5	6.5	7.0	9.0
14.5	5.5	16.0	20.5	19.0	1.0
14.5	2.5	10.0	14.0	4.5	14.0
7.0	8.0	12.0	4.0	4.5	20.0
18.5	8.0	16.0	11.5	14.5	6.0
1.5	4.0	6.5	17.5	2.5	21.0
7.0	17.5	14.0	19.0	21.0	4.0
7.0	17.5	3.5	1.0	2.5	13.0
7.0	15.0	1.0	4.0	1.0	10.0
14.5	11.0	18.5	11.5	16.5	5.0
20.5	5.5	16.0	11.5	14.5	11.0
7.0	17.5	2.0	6.5	6.0	15.0
7.0	13.0	20.0	17.5	20.0	8.0
14.5	14.0	12.0	11.5	16.5	17.0
7.0	20.0	6.5	4.0	9.5	19.0